nature metabolism

Article

https://doi.org/10.1038/s42255-024-01194-6

Separate orexigenic hippocampal ensembles shape dietary choice by enhancing contextual memory and motivation

Received: 23 October 2023

Accepted: 28 November 2024

Published online: 15 January 2025

Check for updates

Mingxin Yang[1,2], Arashdeep Singh[1,2], Alan de Araujo[1,2], Molly McDougle[1,2], Hillary Ellis[1,2], Léa Décarie-Spain[3], Scott E. Kanoski[3] & Guillaume de Lartigue[1,2]

The hippocampus (HPC) has emerged as a critical player in the control of food intake, beyond its well-known role in memory. While previous studies have primarily associated the HPC with food intake inhibition, recent research suggests a role in appetitive processes. Here we identified spatially distinct neuronal populations within the dorsal HPC (dHPC) that respond to either fats or sugars, potent natural reinforcers that contribute to obesity development. Using activity-dependent genetic capture of nutrient-responsive dHPC neurons, we demonstrate a causal role of both populations in promoting nutrient-specific intake through different mechanisms. Sugar-responsive neurons encoded spatial memory for sugar location, whereas fat-responsive neurons selectively enhanced the preference and motivation for fat intake. Importantly, stimulation of either nutrient-responsive dHPC neurons increased food intake, while ablation differentially impacted obesogenic diet consumption and prevented diet-induced weight gain. Collectively, these findings uncover previously unknown orexigenic circuits underlying macronutrient-specific consumption and provide a foundation for developing potential obesity treatments.

Survival hinges upon the acquisition of sufficient food to meet metabolic demands. Therefore, being able to construct a cognitive map and navigate accurately to a known food source in the environment confers a distinct competitive advantage. Animals learn to use contextual cues linked to the nutritional value of food[1] and form episodic memories of the spatial location of cues to enable efficient return to previously encountered food sources. Repeatedly associating discrete or contextual cues with food in a manner that predicts food intake induces a motivational state that amplifies the desire to eat—a phenomenon termed cue-potentiated eating[2]. This adaptive behavior becomes overwhelmed in our current food environment, which is characterized by an inundation of food-associated cues and readily-available foods rich in fats and sugars. Associative-learning mechanisms linking food cues with intake of calorie-dense diets amplifies susceptibility to obesity development. Supporting this notion, brain reactivity to food cues in people predicts current body mass index[3], the inclination to gain weight in the future[4,5], and food choice[6,7]. Hence, unraveling mechanisms governing memory formation regarding contextual cues linked to fat and sugar intake holds potential for combating obesity.

The hippocampus (HPC) is a neural substrate that is critical for cognitive mapping[8] and the formation of episodic memories related to autobiographical experiences and their contextual details[9,10]. Given the pivotal role of navigational and contextual memory in acquiring food, it is not surprising that recent evidence suggests that the HPC also has

[1]Monell Chemical Senses Center, Philadelphia, PA, USA. [2]Department of Neuroscience, Perelman School of Medicine, University of Pennsylvania, Philadelphia, PA, USA. [3]Human & Evolutionary Biology Section, Department of Biological Sciences, University of Southern California, Los Angeles, CA, USA. e-mail: gdelartigue@monell.org

a role in the control of food intake[11,12]. Specifically, the HPC becomes activated by post-ingestive signals following a mixed meal[13], hormones released from the gut in response to eating[13], and sensory cues associated with meals, including odors[14,15], taste[16,17], texture[18], tones[19], and visual cues[20]. Lesioning of the HPC in rats leads to an increase in food intake[21] and body weight in both females[22] and males[11]. Conversely, chemogenetic stimulation of glutamatergic HPC neurons inhibits 24-h food intake[23]. People with retrograde amnesia resulting from brain lesions that encompass the HPC consume multiple successive meals[24,25], which can be interpreted as impaired memory or impaired sensing of internal metabolic needs, an outcome that has also been observed in rodents with HPC lesions[26,27]. Disruption of HPC function has also been associated with obesity. In a human functional magnetic resonance imaging (fMRI) study, hippocampal blood flow was lower after a meal in individuals with obesity than in those with a healthy weight[28]. Feeding rats a high-fat, high-sugar diet impairs performance on hippocampal-dependent spatial learning and episodic memory tasks[29]. Taken together, these data highlight the HPC as having an anorexigenic role in energy metabolism, with mechanisms involving episodic memory[30,31], spatial memory[32], and appetitive reward[26,33].

The HPC has also been found to be activated in conditions associated with increased food intake. When administered into the HPC of rats, ghrelin, an orexigenic hormone released from the stomach under fasting conditions[34], increases food intake and motivation to work for a sugar reward[35]. In human fMRI studies, HPC activity is enhanced in response to images of food and tastants[36,37], shown to promote arousal and motivation to eat[38,39], and these effects are strongest in individuals with obesity. Recent findings have identified an HPC subregion in humans as a key hub for encoding the appetitive value of sugar and fat, with a compromised HPC appetitive subnetwork in individuals with obesity[40]. These data suggest a potential role for the HPC in increasing food intake, although the existence of a specific orexigenic population of HPC neurons remains unproven. This knowledge gap could partly stem from limitations in the temporal and spatial resolution of previous studies using lesions and pharmacological approaches. The dorsal HPC (dHPC) has been understudied, despite recent advances in transcriptomic analyses that have unveiled extensive molecular diversity in dHPC neurons[41–44] and ongoing efforts to functionally characterize subpopulations on the basis of their projection patterns and/or genetic markers[45]. Notably, screening of meal-responsive neurons revealed that a substantial number of neurons in the dHPC are activated by eating[23]. A fraction of these meal-responsive neurons have been identified as DRD2-expressing neurons in the dHPC hilar region, and molecular and genetic tools have been demonstrated to inhibit food intake[23]. We hypothesized that fat and sugar might activate a subset of HPC neurons with orexigenic function. Our results find subsets of HPC neurons that are recruited in response to fats or sugars, and leverage Fos^{TRAP} mice as an unbiased approach to manipulate the activity of these HPC neurons to test their role in appetitive behavior.

Results

Post-ingestive nutrient signals engage the HPC through vagal pathways

Previous studies have demonstrated that the HPC is activated in response to mixed nutrient chow[23] and following intragastric (IG) infusion of a mixed meal[13]. To test whether the HPC is activated in response to individual nutrients, we measured Fos immunofluorescence, a marker of neuronal activity, in mildly fasted wild-type mice in response to IG infusions (500 µl, 100 µl min^{-1}) of sugar (sucrose, 15% wt/vol), equicaloric fat (microlipid, 6.8% vol/vol), or isosmotic saline (0.9% wt/vol) (Fig. 1a). The Fos level was increased in discrete neuronal populations in the dHPC in mice that received infusions of sucrose or fat, compared with the Fos level in those that received saline (Fig. 1b). Similar Fos density was found in response to both nutrients throughout the dHPC (Fig. 1c–e), but the density of sucrose- or fat-responsive neurons was particularly enriched in the dentate gyrus (DG) (Fig. 1c) compared with the CA3 (Fig. 1d) and CA1 (Fig. 1e). Notably, IG infusions of sucrose and fat also resulted in a similar density of Fos labeling in the ventral HPC (vHPC) (Extended Data Fig. 1a–e), but unlike the dHPC, this region was particularly enriched in the CA1 (Extended Data Fig. 1f–i). Together, these data highlight that HPC neurons are responsive to post-ingestive nutrient signals from the gut.

The vagus nerve is a key neural pathway that connects the gut and the brain. Subsets of vagal sensory neurons in the nodose ganglia (NG) respond to intestinal nutrients, and are necessary to mediate the reinforcing value of fat and sugar[46]. Vagal sensory fibers terminate in the nucleus tractus solitarius (NTS) of the hindbrain, and evidence suggests that a polysynaptic circuit links the gut through the NTS to the HPC[47]. Furthermore, deleting gut-innervating vagal sensory neurons impairs HPC-dependent contextual episodic memory[47,48]. To investigate whether the vagus nerve is required for post-ingestive fats and/or sugars to activate dHPC neurons, we measured Fos expression in the dHPC after IG nutrient infusions in mice with subdiaphragmatic vagotomy or that underwent sham surgery (Fig. 1f). Control mice with intragastric saline infusion showed low dHPC Fos levels (Fig. 1g), which increased in response to either sucrose (Fig. 1h,i) or fat (Fig. 1j,k). Nutrient-induced dHPC Fos expression was significantly reduced in animals with subdiaphragmatic vagotomy (Fig. 1h–k), indicating the vagus nerve is at least partially necessary to relay gut-derived nutrient signals to the dHPC.

To further assess the gut–hippocampus connection, we measured dHPC cFos labeling after optogenetic stimulation of nutrient-responsive vagal sensory neurons. We used Fos^{TRAP} mice[49,50], allowing targeted recombination in active populations (Fig. 1l). These mice express an inducible Cre recombinase, driven by an activity-dependent Fos promoter, enabling permanent genetic access to activated neurons upon injection of 4-hydroxytamoxifen (4-OHT)[51–53]. We crossed the Fos^{TRAP} mice with a Cre-dependent tdTomato reporter line, Ai14 (ref. 54). To stimulate nutrient-responsive vagal sensory

Fig. 1 | Dorsal hippocampus encodes gut-derived nutrient signals through a vagal pathway. a, Schematic of Fos staining approach to assess dHPC neuronal responsiveness to IG infusions of saline, sugar (15% wt/vol sucrose), or fat (6.8% vol/vol microlipid). **b**, Representative images of Fos expression in the dHPC from 5 animals per group. **c**–**e**, Quantification of Fos-positive neurons in the dorsal dentate gyrus (dDG) (**c**), CA3 (**d**), and CA1 (**e**) following IG saline, sugar, or fat infusions ($n = 5$ mice per group, ordinary one-way analysis of variance (ANOVA) with Tukey post-hoc analysis). **f**, Schematic of subdiaphragmatic vagotomy (VGX) to assess the role of the vagus nerve in dHPC neuronal nutrient sensing. **g**,**h**, Representative images of Fos expression in dDG from sham (**g**) or VGX (**h**) mice receiving IG saline or sugar (images representative of experiments from 5–6 animals). **i**, Quantification of dHPC Fos expression in response to sugar with or without VGX compared to saline control ($n = 5$ for Saline^{Sham} and Sugar^{Sham}, $n = 6$ for Sugar^{VGX}, ordinary one-way ANOVA with Tukey post-hoc analysis). **j**,**k**, Representative images (**j**) and quantification (**k**) of Fos expression in the dHPC following IG fat infusion with or without VGX, using the same sham saline control data as in **i** ($n = 5$ for Saline^{Sham} and Fat^{VGX}, $n = 7$ for Fat^{Sham}, ordinary one-way ANOVA with Tukey post-hoc analysis). **l**, Schematic of optogenetic stimulation of nutrient-responsive vagal sensory neurons in Fos^{TRAP} mice. **m**, Representative images of vagal sensory neurons from Fos^{TRAP} mice bilaterally injected in nodose ganglia with AAV9-DIO-ChR2-eYFP (cyan) and coexpressed in tdTomato^{+} neurons trapped following IG nutrient infusion (magenta) (images representative of experiments from 6–8 animals). **n**, Representative images of Fos expression in the dDG following vagal optogenetic stimulation in control, Sugar^{TRAP}, and Fat^{TRAP} mice in independent experiments involving 6–8 mice. **o**, Quantification of dHPC Fos expression in response to optogenetic stimulation of nutrient-sensing NG neurons ($n = 6$ for control and Sugar^{ChR}, $n = 8$ for Fat^{ChR}, ordinary one-way ANOVA with Tukey post-hoc analysis). Data are presented as mean ± s.e.m. Scale bars, 100 µm. SO, stratum oriens; SP, stratum pyramidale; SR, stratum radiatum; ML, molecular layer; GCL, granule cell layer. Elements of **a**, **f**, and **l** were created in Biorender.

https://doi.org/10.1038/s42255-024-01194-6

neurons, we injected the NG with the Cre-inducible viral construct AAV9-EF1a-DIO-hChR2(H134R)-EYFP[55] to selectively express the light-sensitive depolarizing channelrhodopsin-2 (ChR2) in these neurons (Fig. 1l). As previously validated[46], 2 weeks after viral injection, fasted Fos^{TRAP} mice received IG infusions (500 µl at 100 µl min^{-1}) of either sucrose (15% wt/vol) or equicaloric fat (microlipid, 6.8% vol/vol), followed by 4-OHT (30 mg kg^{-1}) intraperitoneally (i.p.). We confirmed high overlap between Fos^{TRAP} labeling (tdTomato^{+}) and ChR2 expression in NG neurons (Fig. 1m). Optogenetic activation of either the fat- or sucrose-sensing NG population induced robust cFos expression in the

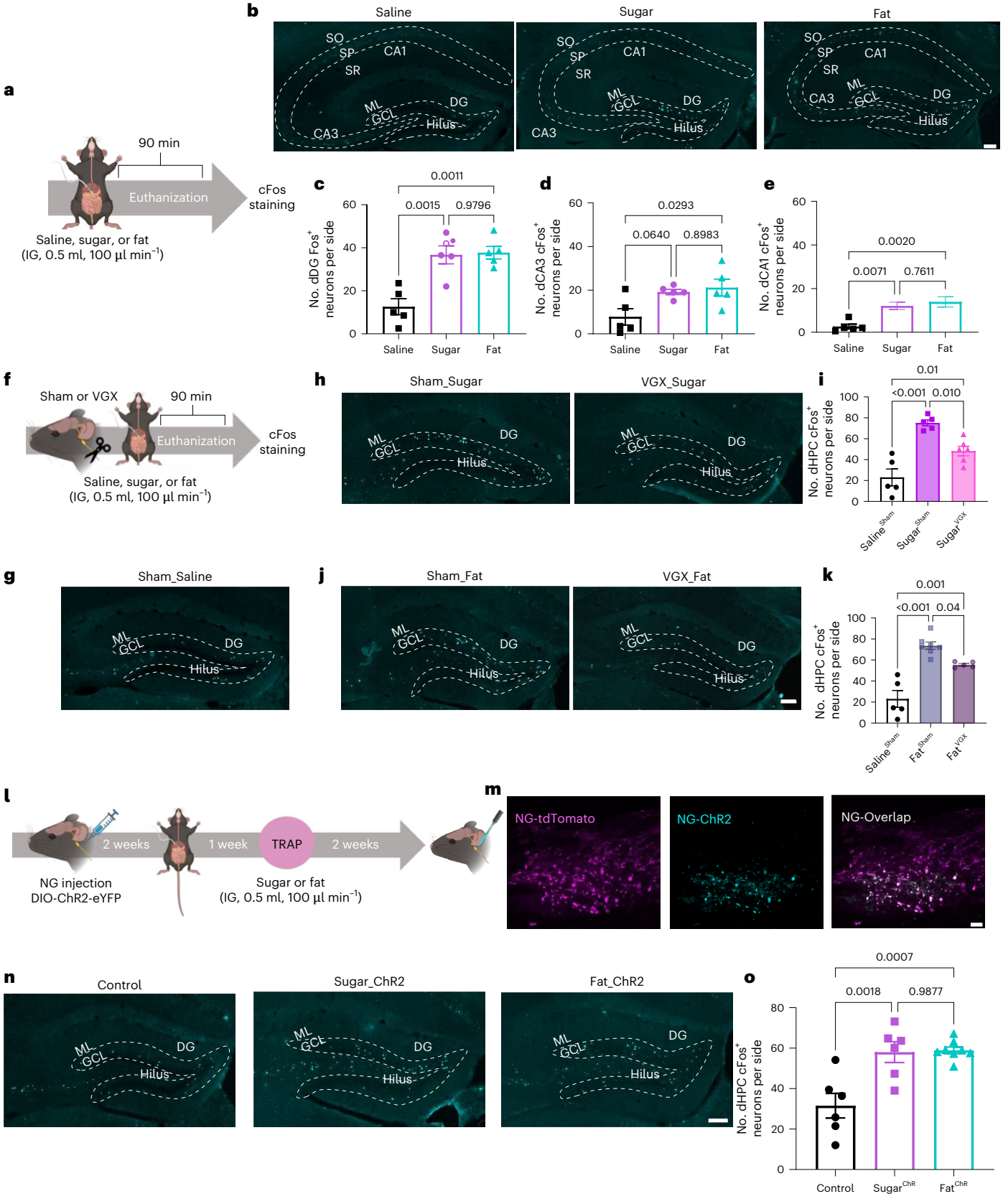

dHPC (Fig. 1n,o). These findings reveal a functional gut–dHPC connection, and that vagal sensory neurons are both necessary and sufficient for transmitting nutrient-specific signals to the hippocampus.

Distinct dorsal hippocampal ensembles for fat and sugar

We recently reported that nutrients activate parallel but separable gut–brain circuits[46]. Thus, to determine whether the dHPC contains distinct neuronal populations that are responsive to fat and sugar, we employed a Fos^{TRAP} mouse using a previously validated approach[46] to compare neuronal activity following two nutrient infusions in the same mouse (Fig. 2a). Validation confirmed that the number of dHPC neuronal responses was similar between Fos^{TRAP} tdTomato and Fos immunofluorescence in response to sucrose (Extended Data Fig. 2a) or fat (Extended Data Fig. 2b). High immunofluorescence overlap between Fos^{TRAP} tdTomato and Fos^{+} neurons in response to IG fat (Fat^{Fos}) in the dHPC (Fig. 2b,c), indicated consistent neuronal activation to repeated fat infusions. However, when comparing the response to different stimuli, there was little overlap between Fos^{TRAP} tdTomato with IG sugar and Fat^{Fos} labeling demonstrated distinct neuronal populations were activated following consumption of different nutrients (Fig. 2b,c). This differentiation was particularly pronounced in the DG (Extended Data Fig. 2c), consistent with the role of the DG as a pattern segregator[50–53]. Importantly, neither fat nor sucrose activated hilar neurons, distinguishing these populations from previously described DRD2-expressing satiety neurons[23].

Our results identify two previously uncharacterized populations of dHPC neurons that are differentially responsive to post-ingestive fats and sugars. To characterize these neurons, we examined neurotransmitter phenotypes using in situ hybridization for vesicular glutamate transporter 1 (vGLUT1) and gamma-aminobutyric acid (GABA). GABA neurons were primarily restricted to the hilar region of the dHPC (Fig. 2d). We found GABA expression in less than 5% of fat- or sugar-responsive dHPC neurons (Fig. 2e). Conversely, we found that vGLUT1 extensively labeled neurons throughout the dHPC (Fig. 2f). The majority of the fat- and sugar-responsive dHPC neurons colocalized with vGLUT1 (Fig. 2g). Our findings indicate that both populations are predominantly glutamatergic, although it is important to note that these neurons represent only a small fraction of the overall glutamatergic population in the dHPC (Extended Data Fig. 2d,e). These findings reveal that the dHPC contains distinct, glutamatergic neuronal populations that selectively encode post-ingestive fat and sugar signals, suggesting a potential neural basis for macronutrient-specific choice.

dHPC neurons control nutrient-specific preference and intake

Next, we wanted to determine the role of nutrient-responsive dHPC populations in the control of food intake, and reasoned that these spatially segregated populations recruited by separate post-ingestive nutrients could differentially resolve food intake at the macronutrient level[56,57]. We genetically targeted the distinct populations activated by IG fat or sucrose in Fos^{TRAP} mice (Fig. 3a). Subsequently, we selectively ablated these neurons using a cre-dependent virus expressing caspase (AAV-flex-taCasp3-TEVp) or a control virus[58]. To assess the efficacy of the Casp3-mediated ablation strategy, we quantified the tdTomato-positive neurons in the dHPC. Casp3-treated mice had less than 50% of the tdTomato-positive dHPC neurons of control mice (Fig. 3b–d). This result demonstrates the successful ablation of sugar- and fat-responsive neurons. To confirm the specificity of the viral targeting, we quantified the number of tdTomato-positive neurons in the paraventricular hypothalamus (PVH), and found no differences in both sucrose (Extended Data Fig. 3a,b) and fat (Extended Data Fig. 3c,d) conditions, indicating that the Casp3 virus specifically targeted dHPC neurons without affecting overall Fos^{TRAP} expression. To evaluate the role of these dHPC neurons in nutrient preference, we presented the mice with a choice between two bottles containing equicaloric solutions of sugar (15%) or fat (6.8%) and quantified their intake using lickometers (Fig. 3a). Over 3 test days, the control mice exhibited a preference for the fat solution over the sucrose solution (Fig. 3e–h). The mice with ablated sugar-responsive dHPC neurons exhibited a 50% decrease in sucrose consumption compared with controls (Fig. 3e), with no effect on fat intake (Fig. 3f). Deletion of fat-responsive dHPC neurons resulted in no change in sucrose intake (Fig. 3g), but reduced fat consumption by 40% compared with that of control mice (Fig. 3h). To assess the potential influence of taste preferences on food intake, we conducted brief-access taste tests. No significant differences in licking behavior were observed between groups across a range of sucrose and fat concentrations (Extended Data Fig. 4a–e), confirming that taste preferences did not underlie the observed macronutrient selectivity. When the bottles were presented one at a time in a one-bottle test, deletion of sucrose-responsive dHPC neurons had no effect on sucrose or fat intake, suggesting that these neurons influence choice rather than intake (Extended Data Fig. 4f,g). Ablation of dHPC^{Fat} neurons had no effect on sucrose intake in a one-bottle test (Extended Data Fig. 4h), but reduced the number of licks for fat (Extended Data Fig. 4i), suggesting that these neurons influence both choice and intake of fat. In summary, separate populations of dHPC neurons are necessary for post-ingestive nutrient-specific preference.

To determine whether activation of dHPC neurons alone is sufficient to influence macronutrient intake, we performed chemogenetic stimulation of fat- or sugar-responsive dHPC neurons. A Cre-inducible viral Gq-coupled designer receptor (AAV-EF1a-DIO-hM3Dq-mCherry)[59] was bilaterally injected into the dHPC of Fos^{TRAP} mice (Fig. 3i). Clozapine *N*-oxide (CNO) administration induced Fos expression in dHPC neurons of both Sugar^{TRAP} and Fat^{TRAP} mice compared with controls (Extended Data Fig. 4j and l), and resulted in significant overlap of Fos in the TRAP neurons (Fig. 3j and Extended Data Fig. 4k). These findings confirm the successful chemogenetic activation of nutrient-specific dHPC neuronal populations. In the one-bottle test, chemogenetic activation of dHPC^{Sugar} neurons increased sucrose intake compared with vehicle treatment (Fig. 3k) but had no effect on fat intake (Fig. 3l). Stimulation of dHPC^{Fat} neurons exclusively increased fat consumption (Fig. 3m,n). Notably, none of these effects were observed when CNO was injected in mice that did not carry the chemogenetic construct (Extended Data Fig. 4m–o). These data suggest that the dHPC is attuned to specific macronutrients, allowing for highly refined feeding decisions.

dHPC neurons control nutrient-specific spatial memory

Next, we wanted to examine the mechanisms by which dHPC neurons control nutrient-specific intake. The HPC forms context-specific neural representations that provide a physiological substrate of spatial memory[60], and HPC activity is altered by contextual features of

Fig. 2 | Distinct glutamatergic dorsal hippocampal ensembles for fat and sugar. a, Schematic of the Fos^{TRAP} approach comparing tdTomato labeling with Fos labeling in response to IG nutrient infusions. **b**, Representative images of the dDG in Fos^{TRAP} mice following IG infusion of fat or sugar (tdTomato, magenta, top), and 2 weeks later in the same mouse after IG infusion of fat (Fos, cyan; middle). Colocalization of neurons responding to both stimuli (white; bottom) along with a higher magnification image (center). **c**, Quantification of the overlap between neurons responding to repeated fat infusions (fat/fat) compared with infusions of different macronutrients (sugar/fat) in the dHPC. $n = 5$ mice per group, unpaired two-tailed *t*-test. **d**, Images of the dDG showing GABA mRNA expression (cyan) and tdTomato-positive neurons (magenta) in Fos^{TRAP} mice following IG infusion of sugar or fat. **e**, Proportion of tdTomato^{+} neurons colocalized with GABA mRNA. **f**, Images of the dDG showing vGLUT1 mRNA expression (cyan) and tdTomato-positive neurons (magenta) in Fos^{TRAP} mice following IG infusion of sugar or fat. **g**, Proportion of tdTomato^{+} neurons colocalized with vGLUT1 mRNA. Data are presented as mean ± s.e.m. ***$P < 0.001$. All images are representative of independent experiments from 5 animals. Scale bars, 100 µm. Elements of **a** were created in Biorender.

https://doi.org/10.1038/s42255-024-01194-6

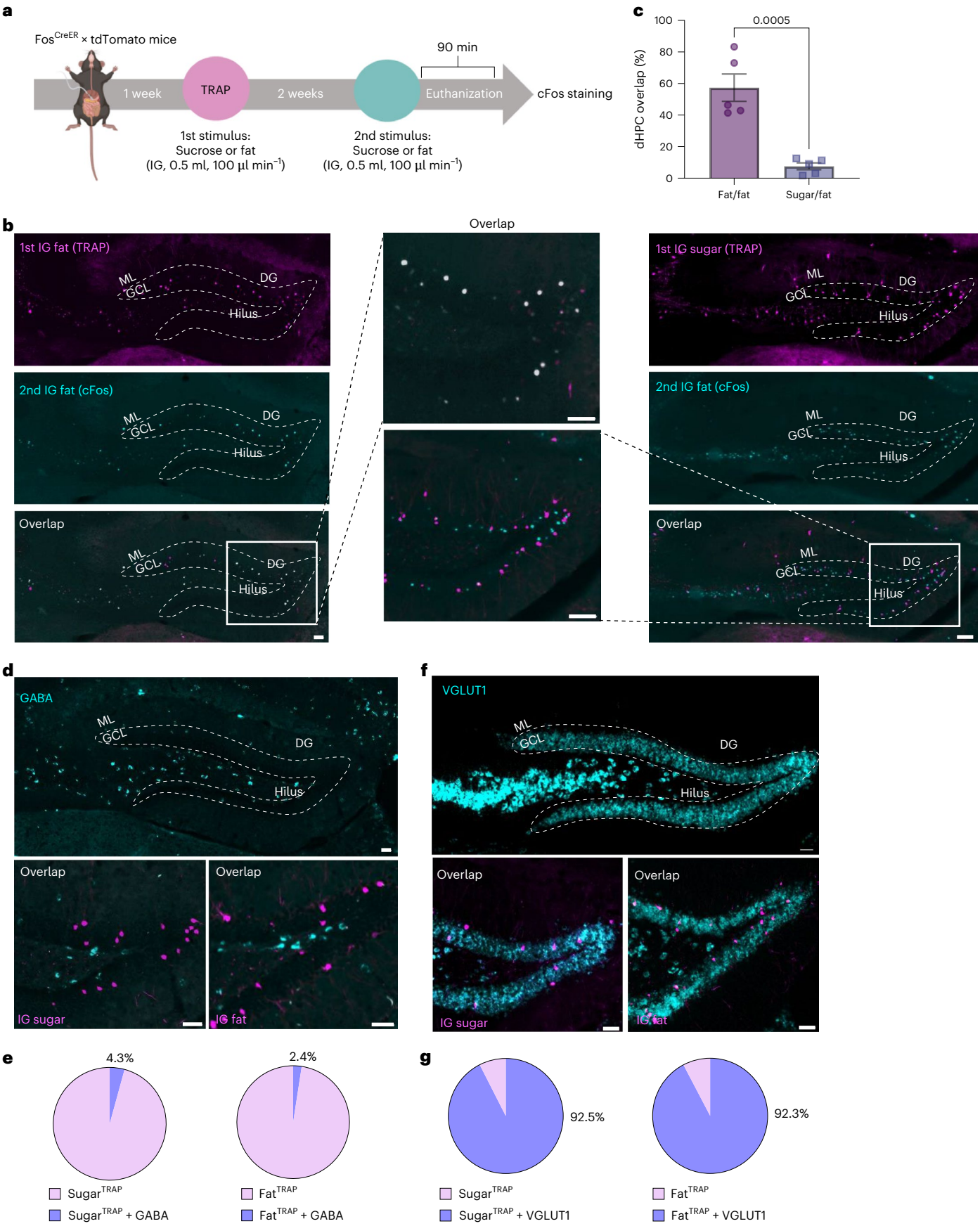

https://doi.org/10.1038/s42255-024-01194-6

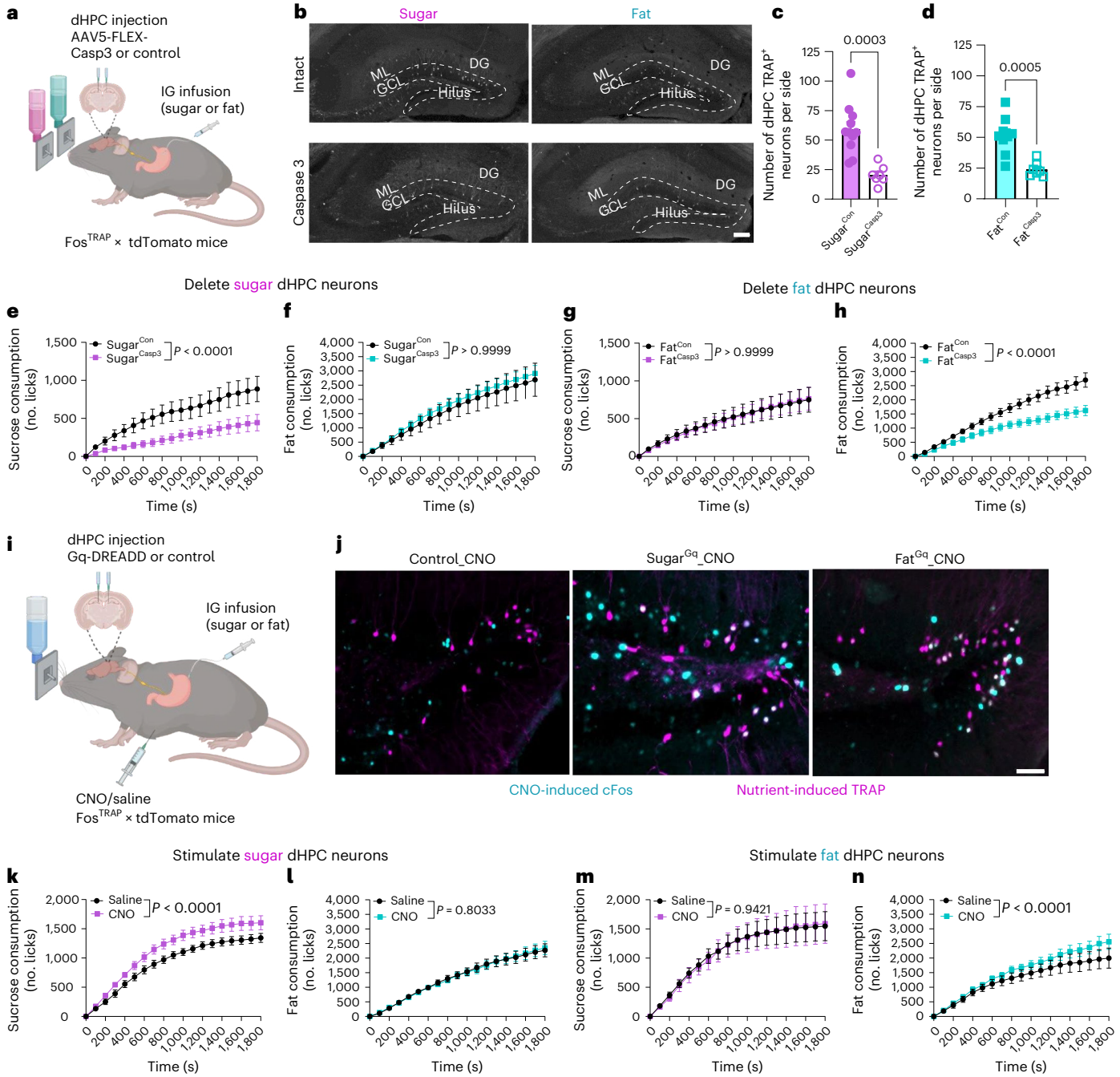

Fig. 3 | Fat- and sugar-responsive dHPC neurons control nutrient-specific preference. a, Schematic of the two-bottle choice test in Fos^{TRAP} mice with selective ablation of nutrient-responsive dHPC neurons responding to IG infusion of sugar or fat. **b**, Representative images of nutrient-responsive HPC neurons from Fos^{TRAP} mice following IG infusion of sugar or fat, with or without caspase ablation. **c**,**d**, Quantification of tdTomato$^+$ neurons in dHPC^{Sugar} mice with and without ablation (n = 11 for Sugar^{Con}, n = 7 for Sugar^{Casp3}, unpaired two-tailed *t*-test) (**c**) or dHPC^{Fat} mice with and without ablation (*n* = 9 for Fat^{Con}, *n* = 7 for Fat^{Casp3}, unpaired two-tailed *t*-test) (**d**). **e**–**h**, Two-bottle choice test intake of sugar and fat. **e**, Sugar licking in dHPC^{Sugar} mice with and without ablation (*n* = 9 mice per group, two-way ANOVA with Holm–Sidak post-hoc analysis). **f**, Fat licking in dHPC^{Sugar} mice with and without ablation (*n* = 8 for Fat^{Con}, *n* = 9 for Fat^{Casp3}, two-way ANOVA with Holm–Sidak post hoc analysis). **g**, Sugar licking in dHPC^{Fat} mice with and without ablation (*n* = 8 mice group, two-way ANOVA with Holm–Sidak post hoc analysis). **h**, Fat licking in dHPC^{Fat} mice with and without ablation (*n* = 8 mice per group, two-way ANOVA with Holm–Sidak post hoc analysis). **i**, Schematic of the Fos^{TRAP} approach to chemogenetically stimulate nutrient-responsive HPC neurons responding to IG infusion of sugar or fat. **j**, Representative images of dDG tdTomato$^+$ neurons (magenta) and CNO-induced Fos expression (cyan) in dHPC^{Sugar} and dHPC^{Fat} mice. **k**–**n**, Effects of chemogenetic stimulation on sugar and fat consumption. **k**, Sugar licking in dHPC^{Sugar} mice with and without hM3Dq (*n* = 8 mice per group, two-way within-subjects ANOVA with Holm–Sidak post-hoc analysis). **l**, Fat licking in dHPC^{Sugar} mice with and without hM3Dq (*n* = 7 mice per group, two-way with-subjects ANOVA with Holm–Sidak post hoc analysis). **m**, Sugar licking in dHPC^{Fat} mice with and without hM3Dq (*n* = 7 mice per group, two-way within-subjects ANOVA with Holm–Sidak post hoc analysis). **n**, Fat licking in dHPC^{Fat} mice with and without hM3Dq (*n* = 6 mice per group, two-way within-subjects ANOVA with Holm–Sidak post hoc analysis). Data are presented as mean ± s.e.m. Images are representative of independent experiments from 7–11 (**b**) or 5–6 animals (**j**). Scale bars, 100 µm. Elements of **a** and **i** were created in Biorender.

rewarding stimuli[61–63]. To address whether dHPC^{Sugar} and dHPC^{Fat} neurons retain contextual information about the location of natural reinforcers, such as post-ingestive fats and sugars, we adapted a food-cup location memory task[23]. Mice were habituated to a novel context with two empty Petri dishes, and during the training phase, one Petri dish contained droplets of water, whereas the other contained droplets of fat or sucrose solutions (Fig. 4a). After training to learn the location of a nutrient-containing dish, we used empty Petri dishes to test the mice in the same context to determine whether they could remember the location of the nutrient-paired quadrant (Fig. 4a). Control mice discriminated the sugar-paired quadrant above chance in tests conducted 1 h and 24 h after the final training session (Fig. 4b), suggesting that they could learn and remember the location of sucrose. Mice with ablated dHPC^{Sugar} neurons failed to discriminate the location of the sugar dish in the 1 h and 24 h tests (Fig. 4c). However, when these mice repeated the task with a fat solution using different contextual cues, there were no group differences in exploration of the fat location at either time point (Extended Data Fig. 5a,b). In a separate group of Fos^{TRAP} mice trapped with IG infusion of fat, we found that controls and dHPC^{Fat} ablated mice could discriminate the sugar location in both 1 h and 24 h tests, compared with their pre-test performance (Extended Data Fig. 5c,d). Although the control mice exhibited fat location memory (Fig. 4d), the ablation of fat-responsive dHPC neurons abolished the ability to discriminate the fat-paired location in both 1 h and 24 h tests (Fig. 4e). Notably, the order in which the nutrients were presented was counterbalanced, and there was no residual preference for the previous nutrient location following a 7-day washout period (Extended Data Fig. 5e), indicating a preference for exploring the new Petri dish locations.

To determine whether generalized spatial memory is impaired, we performed a hippocampal-dependent[64] novel object in context (NOIC) task (Extended Data Fig. 5f). As expected, control mice spent more time exploring the object that is novel to the context (Extended Data Fig. 5g–j). The ablation of either fat- or sugar-responsive dHPC neurons had no effect on the time spent exploring the novel object (Extened Data Fig. 5g–j). These data indicate that the loss of nutrient-responsive dHPC neurons influences contextual memory of nutrient location, and that these neurons are specific to food with no impact on contextual memory for non-food-related objects.

Increasing evidence suggests that the HPC is involved in spatial working memory[65,66], which allows retention of a small amount of information for a short period of time. To assess whether the nutrient-responsive dHPC neurons influence working memory related to food location, we performed a modified Barnes maze task[47]. Mice were positioned in the center of a circular table, and 16 Petri dishes containing water solution and one containing either sucrose (15% wt/vol) or equicaloric fat (6.8% vol/vol) were evenly distributed around the edge (Extended Data Fig. 6a). The location of the nutrient-containing dish remained the same across two consecutive trials per day, but was changed each subsequent day (Extended Data Fig. 6a). The index of working memory on this task is the difference in the number of errors (exploration of water dishes) between trials on 3 individual experimental days. We observed no difference in the number of errors in response to either nutrient in mice with ablation of dHPC^{Sugar} (Extended Data Fig. 6b–e) or dHPC^{Fat} (Extended Data Fig. 6f–i) neurons, suggesting that ablation of nutrient-responsive dHPC neurons does not have a role in spatial working memory. Altogether, these data suggest that both fat- and sugar-responsive dHPC neurons are uniquely necessary for episodic spatial reference memory for the location of individual nutrients.

Next, we assessed whether activation of nutrient-responsive dHPC neurons can promote context-dependent spatial recall for individual nutrients. Mice expressing hM3Dq or control virus in dHPC neurons trapped with IG infusion of either sucrose (15% wt/vol) or fat (6.8% vol/vol) were habituated to two novel contexts. During a 3-day training phase, the mice received saline injections 20 minutes before being placed in context A in the morning, where they had 10 minutes to learn to associate the location of a nutrient-containing dish. They then received another saline injection before being placed in context B in the afternoon, where they learned a different location for the second nutrient-containing dish. Twenty-four hours later, the mice were tested to determine whether they could discriminate the correct context-specific nutrient-paired quadrant (Fig. 4f). The mice failed to discriminate context-specific locations of sucrose or fat when treated with saline (Fig. 4g,h). After 7 days, the same test was repeated, but the mice received CNO (3 mg kg^{-1}, i.p.) during the test day, before they were reintroduced into the context that had been previously paired with the specific nutrient with which they were initially trapped. We found that CNO had no impact on the performance of control mice (Fig. 4g,h); however, chemogenetic stimulation of dHPC^{Sugar} neurons improved the discrimination for the sugar location compared with vehicle treatment (Fig. 4g), and negatively impacted fat location memory (Extended Data Fig. 6j). No effect was observed in response to chemogenetic stimulation of dHPC^{Fat} neurons (Fig. 4h and Extended Data Fig. 6k). These data indicate that sugar-responsive dHPC neurons encode an engram of spatial and context-dependent memory for sugar.

To assess the role of memory in nutrient preference, we modified the two-bottle choice test (Fig. 3a) by randomly swapping bottle locations every 10 minutes (Fig. 4i). In mice with ablation of dHPC^{Fat} neurons, fat consumption remained lower than in controls (Fig. 4j). By contrast, mice lacking dHPC^{Sugar} neurons failed to exhibit a similar reduction in sucrose intake when bottle locations were randomized (Fig. 4k), suggesting that these neurons are critical for using location-based memory to guide food choice. This provides direct evidence for a causal relationship between memory and sucrose intake.

Dorsal hippocampus encodes fat-specific motivation and reward

Dietary preferences are largely learned[67] through reward-based associations[46,51,67,68]. To investigate the role of nutrient-specific dHPC neurons in this process, we used a flavor-nutrient conditioning task (Fig. 5a)[69]. Control mice developed conditioned preferences for both sucrose and fat (Fig. 5b). Ablation of dHPC^{Sugar} neurons did not impair the acquisition of flavors associated with either nutrient (Fig. 5c), but

Fig. 4 | Fat- and sugar-responsive dHPC neurons control nutrient-specific episodic spatial memory. a, Schematic of nutrient-driven location memory task to assess the necessity of nutrient-responsive dHPC neurons in food-related reference memory. **b**, Discrimination of sugar quadrant in dHPC^{Sugar} mice without viral-mediated ablation (n = 10 mice per group, repeated measure (RM) one-way ANOVA with Dunnett post hoc analysis). **c**, Discrimination of sugar quadrant in dHPC^{Sugar} mice with viral-mediated ablation (n = 7 mice per group, RM one-way ANOVA with Dunnett post hoc analysis). **d**, Discrimination of fat quadrant in dHPC^{Fat} mice without viral-mediated ablation (n = 10 mice per group, RM one-way ANOVA with Dunnett post hoc analysis). **e**, Discrimination of fat quadrant in dHPC^{Fat} mice with viral-mediated ablation (n = 7 mice per group, RM one-way ANOVA with Dunnett post hoc analysis). **f**, Schematic of nutrient-driven location memory task to assess whether chemogenetic stimulation of nutrient-responsive dHPC neurons can promote nutrient-specific recall. **g**, Discrimination of sugar quadrant in response to saline and CNO in dHPC^{Sugar} mice expressing viral-mediated hM3Dq or control (n = 6 for Sugar^{Con}, n = 8 for Sugar^{Gq}, paired two-tailed t-test). **h**, Discrimination of fat quadrant in response to saline and CNO in dHPC^{Fat} mice expressing viral-mediated hM3Dq or control (n = 6 for Fat^{Con}, n = 7 for Fat^{Gq}, paired two-tailed t-test). **i**, Schematic of two-bottle choice test in which bottle positions were swapped every 10 min to assess the importance of location memory on nutrient preference. **j**, Fat licking in dHPC^{Fat} mice with and without ablation (n = 6 for Fat^{Con}, n = 8 for Fat^{Casp3}, two-way ANOVA with Holm–Sidak post hoc analysis). **k**, Sugar solution licking in dHPC^{Sugar} mice with and without viral-mediated ablation (n = 6 for Sugar^{Con}, n = 5 for Sugar^{Casp3}, two-way ANOVA with Holm–Sidak post hoc analysis). Data are presented as mean ± s.e.m. Elements of **a**, **f**, and **i** were created in Biorender.

https://doi.org/10.1038/s42255-024-01194-6

disrupted the subsequent retention of the memory for this preference (Fig. 5d,e). Conversely, deletion of dHPC^{Fat} neurons specifically prevented the formation of fat-associated preferences (Fig. 5f), irrespective of the halved infusion frequency (Extended Data Fig. 7a–c). These findings demonstrate distinct and complementary roles for sugar- and fat-responsive dHPC neurons in reward-based learning and memory.

There is evidence that the dHPC is involved in motivation[70]; therefore, we next assessed whether nutrient-responsive dHPC neurons increase the motivation for food. Effort-based motivation can be tested behaviorally using progressive ratio (PR) schedule reinforcement[71]. We used an exponential PR task to investigate the willingness of mice to lick a dry sipper that requires an increasing number of licks for a small

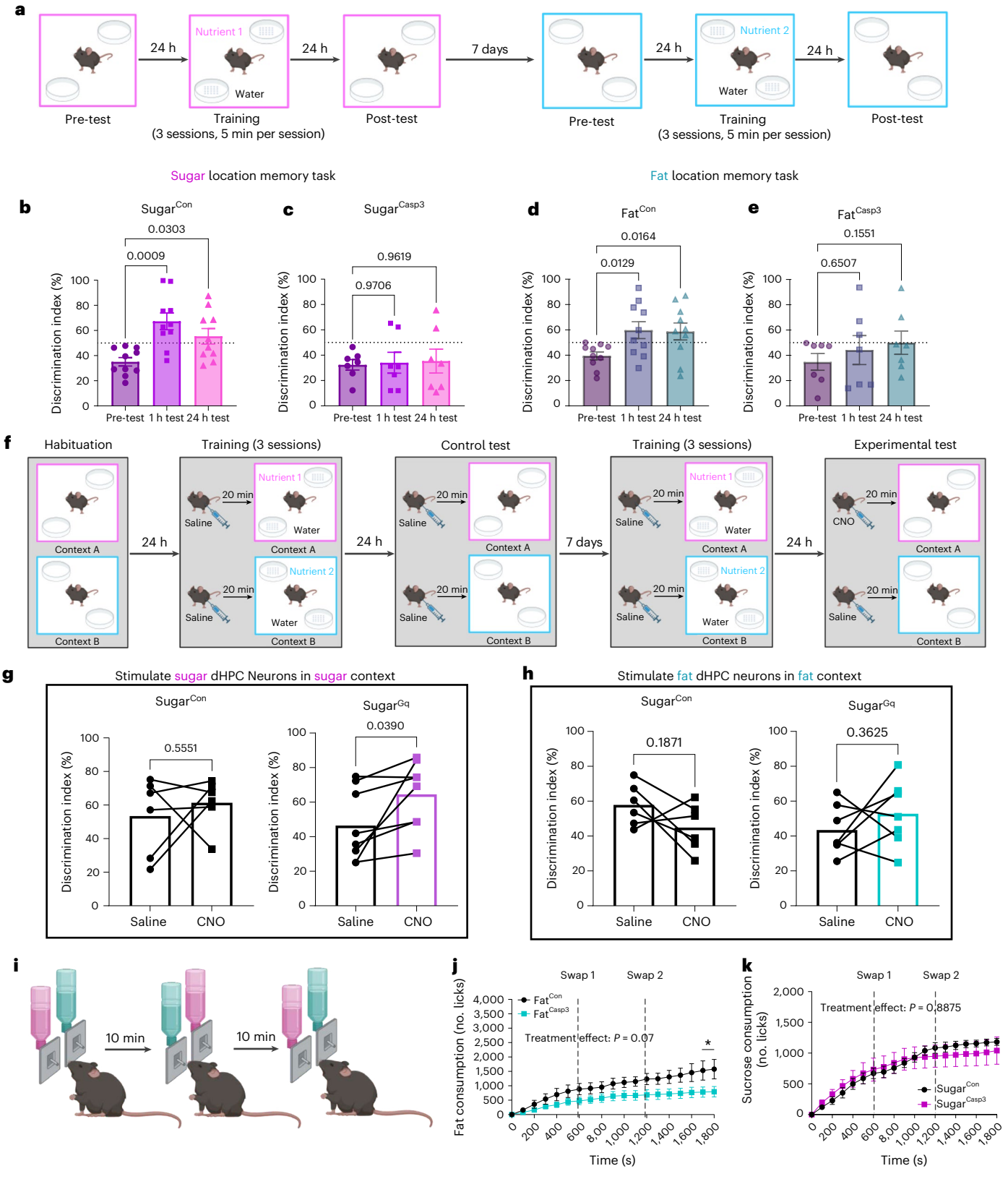

https://doi.org/10.1038/s42255-024-01194-6

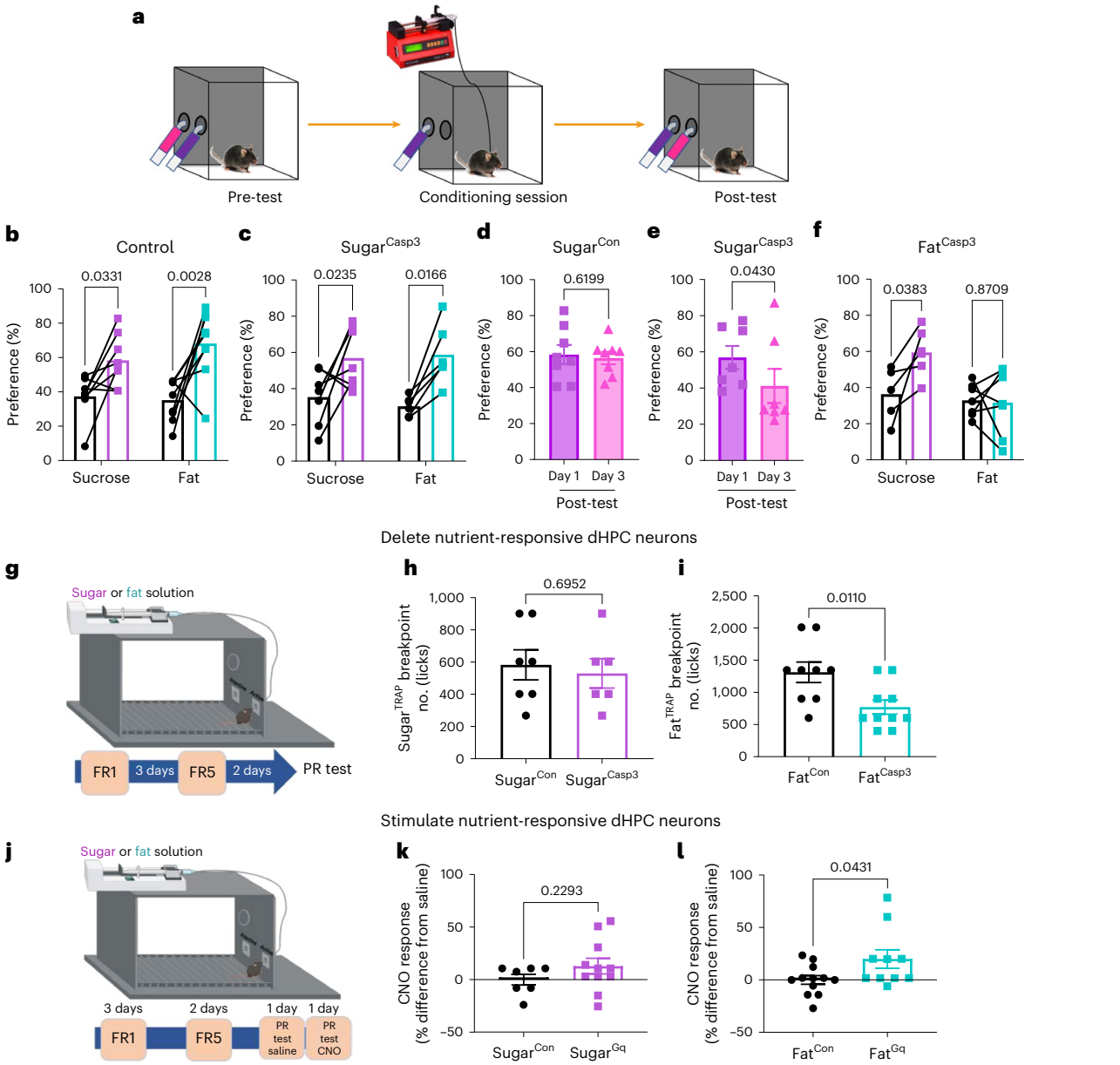

Fig. 5 | Fat-responsive dHPC neurons promote fat reinforcement. a, Schematic representation of the flavor-nutrient conditioning paradigm. **b**, Sugar and fat paired flavor preference pre- and postconditioning in Fos^{TRAP} mice with control virus ($n = 8$ for sugar, $n = 9$ for fat, two-way within-subjects ANOVA with Holm–Sidak post hoc analysis). **c**, Sugar and fat paired flavor preference pre- and postconditioning in Fos^{TRAP} mice with dHPC^{Sugar} ablation ($n = 7$ for sugar, $n = 6$ for fat, two-way within-subjects ANOVA with Holm–Sidak post hoc analysis). **d**, Sugar paired flavor preference on post-test day 1 and 3 in Fos^{TRAP} mice with control virus in dHPC^{Sugar} ($n = 8$ mice per group, paired two-tailed *t*-test). **e**, Sugar paired flavor preference on post-test day 1 and 3 in Fos^{TRAP} mice with dHPC^{Sugar} ablation ($n = 7$ mice per group, paired two-tailed *t*-test). **f**, Sugar and fat paired flavor preference pre- and post-conditioning in Fos^{TRAP} mice with dHPC^{Fat} ablation ($n = 6$ for sugar, $n = 7$ for fat, two-way within-subjects ANOVA with Holm–Sidak post hoc analysis). **g**, Schematic illustration of progressive ratio licking test to assess necessity of nutrient-responsive dHPC in motivation. **h**, Breakpoint for sugar reward in dHPC^{Sugar} mice with control or caspase virus ($n = 7$ for Sugar^{Con}, $n = 6$ for Sugar^{Casp3}, unpaired two-tailed *t*-test). **i**, Breakpoint for fat reward in dHPC^{Fat} mice with control or caspase virus ($n = 9$ for Fat^{Con}, $n = 10$ for Fat^{Casp3}, unpaired two-tailed *t*-test). **j**, Schematic illustration of progressive ratio licking test assessing sufficiency of nutrient-responsive dHPC neurons in motivation. **k**, Breakpoint for sugar reward in dHPC^{Sugar} mice with control or hM3Dq virus ($n = 7$ for Sugar^{Con}, $n = 11$ for Sugar^{Gq}, unpaired two-tailed *t*-test). **l**, Breakpoint for fat reward in dHPC^{Fat} mice with control or hM3Dq virus ($n = 12$ for Fat^{Con}, $n = 10$ for Fat^{Gq}, unpaired two-tailed *t*-test). Data are presented as mean ± s.e.m. Elements of **g** and **j** were created in Biorender.

nutrient reward (Fig. 5g). During the training phase, we observed no group differences in the discrimination for the active side or the number of licks the animals performed under the fixed ratio 1 (FR1) or FR5 ratio (Extended Data Fig. 7d,e). Next we quantified the number of licks required before an animal ceases to be willing to expend effort for a single reward, known as the breakpoint[72]. The willingness of mice with deletion of dHPC^{Sugar} neurons to work for sucrose was not different from that of control mice (Fig. 5h). However, in mice with deletion of dHPC^{Fat} neurons, the breakpoint for fat (Fig. 5i), but not sucrose (Extended Data Fig. 7f,g), was reduced compared with that of control mice, suggesting an important role of dHPC^{Fat} neurons for fat-specific motivation.

Next, we tested whether stimulation of dHPC neurons could increase the motivation to work for nutrients using a similar PR task as above (Fig. 5j). All mice rapidly learned to discriminate the active

nose hole to receive a small nutrient droplet, which was delivered by a pump under both the FR1 and FR5 schedules (Extended Data Fig. 7h,i). After training, the mice were tested on an exponential PR schedule in response to saline or CNO on subsequent days. Compared with saline, CNO (3 mg kg^{-1}, i.p.) had no effect on the sucrose breakpoint in dHPC^{Sugar} control mice or hM3Dq mice (Fig. 5k). However, CNO significantly increased the willingness to nose poke for a small fat reward in the mice expressing hM3Dq in dHPC^{Fat} neurons, but not in controls (Fig. 5l). Notably, CNO alone was not sufficient to promote a place preference independent of nutrient consumption (Extended Data Fig. 8a,b). Notably, the motivational effects of these neurons appear to be specifically tied to food-related contexts, rather than representing a general reward system. Together, these data identify a previously unappreciated population of neurons in the dHPC that are necessary and sufficient to produce the motivation to consume fat.

Deleting orexigenic HPC neurons prevents diet-induced obesity

To investigate the role of nutrient-specific dHPC neurons in regulating energy intake, mice expressing Cre-dependent hM3Dq in either sugar- or fat-responsive dHPC neurons were generated. Mice expressing hM3Dq in sugar-responsive dHPC neurons were acclimated to a high-fat, high-sugar (HFHS) diet for 5 days and received daily saline injections (Fig. 6a). To assess the effects of chemogenetic activation, ad libitum-fed mice received either CNO (3 mg kg^{-1}) or saline injections 30 minutes before the dark phase on alternating days. Food intake was continuously monitored using a BioDAQ system in a home cage setting. Chemogenetic stimulation significantly increased 24-h HFHS diet intake of the mice, compared with saline treatment in the same mice (Fig. 6b). Similarly, mice expressing hM3Dq in dHPC^{Fat} neurons were acclimated to a high-fat (HF) diet for 5 days (Fig. 6c). Chemogenetic stimulation significantly increased 24-h intake of the HF diet (Fig. 6d). These data confirm that both fat- and sugar-responsive dHPC neurons are orexigenic, promoting intake of obesogenic diets.

To assess the necessity of dHPC neurons in regulating energy intake, we generated mice expressing Cre-dependent caspase in sugar-responsive neurons. These mice were fed a HFHS diet for 10 days. Despite similar overall daily intake compared with controls (Fig. 6e), caspase-treated mice exhibited a selective reduction in HFHS consumption during the light phase (Fig. 6f,g), driven by a decrease in meal frequency (Extended Data Fig. 9a,b). Notably, unlike control mice, which gained weight and fat mass over 4 weeks (Fig. 6h,i), caspase-treated mice maintained stable body weight and fat mass (Fig. 6j,k). Between-group comparisons revealed that, at the 4-week timepoint, caspase-treated mice had a significantly lower fat mass than controls (Extended Data Fig. 9c,d). The observed protection against diet-induced obesity aligns with the benefits of time-restricted eating[73,74], suggesting that the decreased meal frequency induced by inhibiting dHPC^{Sugar} neurons may underlie the prevention of weight gain despite unchanged daily food intake. On the basis of the observed role of the dHPC^{Sugar} neurons in food location memory, inhibition of these neurons might impair the recall of food-related memory and promote a time-restricted feeding pattern.

Consistent with the idea that fat- and sugar-responsive neurons have different roles in food intake, caspase ablation of dHPC^{Fat} neurons resulted in a significant reduction in intake of a 60% high-fat diet over 10 days (Fig. 6i). The reduction in food intake was restricted to the dark phase (Fig. 6m,n) and mediated by smaller meal size (Extended Data Fig. 10a). Notably, although control mice exhibited substantial weight gain and increased fat mass after 2 and 4 weeks of consuming a high-fat diet (Fig. 6o–p), caspase-treated mice remained remarkably resistant to diet-induced obesity (Fig. 6q,r). Although between-group analyses did not reveal significant differences in percentage weight gain or fat-mass gain (Extended Data Fig. 10c,d), the marked reduction in food intake and prevention of weight gain in the caspase-treated group highlight the importance of fat-responsive dHPC neurons in promoting energy intake and contributing to diet-induced obesity.

Discussion

In the present study, we demonstrate that the dHPC plays a critical role in controlling food intake. We identify previously unappreciated and distinct orexigenic populations of dHPC neurons that selectively respond to post-ingestive fat or sugar. Although both are orexigenic, they exert differential control over macronutrient preference, motivation, and memory. The dHPC^{Sugar} neurons are essential for spatial memory, whereas dHPC^{Fat} neurons primarily influence motivation. Our findings establish the dHPC as a critical brain region underlying energy balance, with multiple orexigenic neuronal populations representing promising therapeutic targets for obesity intervention.

Identification of orexigenic neurons in the HPC

Prior studies have firmly established the crucial role of an intact HPC in the control of normal eating behavior. Notably, individuals with anterograde amnesia who have lesions that encompass the HPC have shown deficits in the regulation of satiety[25,75,76]. In rodent models, pharmacological lesioning studies in which the entire HPC is removed have demonstrated an increase in food approach behavior[26], meal size[77], and in some cases increased daily food intake and body weight[11,21,22]. Furthermore, transient inhibition of neurons in either the ventral or dorsal HPC has been found to augment food intake[23,30,31,78,79], whereas stimulation of glutamatergic neurons decreases food intake[23,79]. Additionally, the administration of satiety hormones directly into the vHPC has been shown to decrease food intake, whereas the deletion of the receptors for these hormones increases food intake[80,81]. Together, these data support the idea that the HPC plays a causal role in the inhibition of food intake. Yet the HPC is activated by ghrelin[34] and food cues,

Fig. 6 | Sugar-responsive dHPC neurons promote food intake. a, Schematic of experimental paradigm for ad libitum 45% high-fat, high-sugar (HFHS) diet intake from BioDAQ in dHPC^{Sugar} mice expressing either the control or hM3Dq virus. **b**, Cumulative hourly food intake in response to saline or CNO ($n = 6$ mice per group, two-way within-subjects ANOVA with Holm–Sidak post hoc analysis). **c**, Schematic of experimental paradigm for ad libitum 60% high-fat (HF) diet intake from BioDAQ in dHPC^{Fat} mice expressing either the control or hM3Dq virus. **d**, Cumulative hourly food intake in response to saline or CNO ($n = 6$, two-way within-subjects ANOVA with Holm–Sidak post hoc analysis). **e**–**g** dHPC^{Sugar} mice expressing control or caspase virus maintained on HFHS diet for 10 days in BioDAQ. **e**, Ten-day total HFHS diet intake ($n = 10$ for Sugar^{Con}, $n = 9$ for Sugar^{Casp3}, unpaired two-tailed t-test). **f**, Average cumulative HFHS diet intake in dark phase ($n = 11$ for Sugar^{Con}, $n = 12$ for Sugar^{Casp3}, two-way ANOVA with Holm–Sidak post hoc analysis). **g**, Average cumulative HFHS diet intake in light phase ($n = 11$ for Sugar^{Con}, $n = 12$ for Sugar^{Casp3}, two-way ANOVA with Holm–Sidak post hoc analysis). **h**,**i**, Body weight gain (**h**) and fat mass accumulation (**i**) of control mice on HFHS diet for 4 weeks ($n = 9$ mice per group, RM one-way ANOVA with Holm–Sidak post hoc analysis). **j**,**k**, Body weight gain (**j**) and fat mass accumulation (**k**) of dHPC^{Sugar} mice with caspase ablation on HFHS diet for 4 weeks ($n = 9$ mice per group, RM one-way ANOVA with Holm–Sidak post hoc analysis). **l**,**n**, dHPC^{Fat} mice expressing control or caspase virus maintained on HF diet for 10 days in BioDAQ. **l**, Ten-day total HF diet intake ($n = 7$ mice per group, unpaired two-tailed t-test). **m**, Average cumulative HF diet intake in dark phase ($n = 7$ mice per group, two-way ANOVA with Holm–Sidak post hoc analysis). **n**, Average cumulative HF diet intake in light phase ($n = 7$ mice per group, two-way ANOVA with Holm–Sidak post hoc analysis). **o**,**p**, Body weight gain (**o**) and fat mass accumulation (**p**) of control mice on HF diet for 4 weeks ($n = 9$ mice per group, RM one-way ANOVA with Holm–Sidak post hoc analysis). **q**,**r**, Body weight gain (**q**) and fat mass accumulation (**r**) of dHPC^{Fat} mice with caspase ablation on HF diet for 4 weeks ($n = 7$ mice per group, RM One-way ANOVA with Holm–Sidak post hoc analysis). Data are presented as mean ± s.e.m. Elements of **a** and **c** were created in Biorender.

https://doi.org/10.1038/s42255-024-01194-6

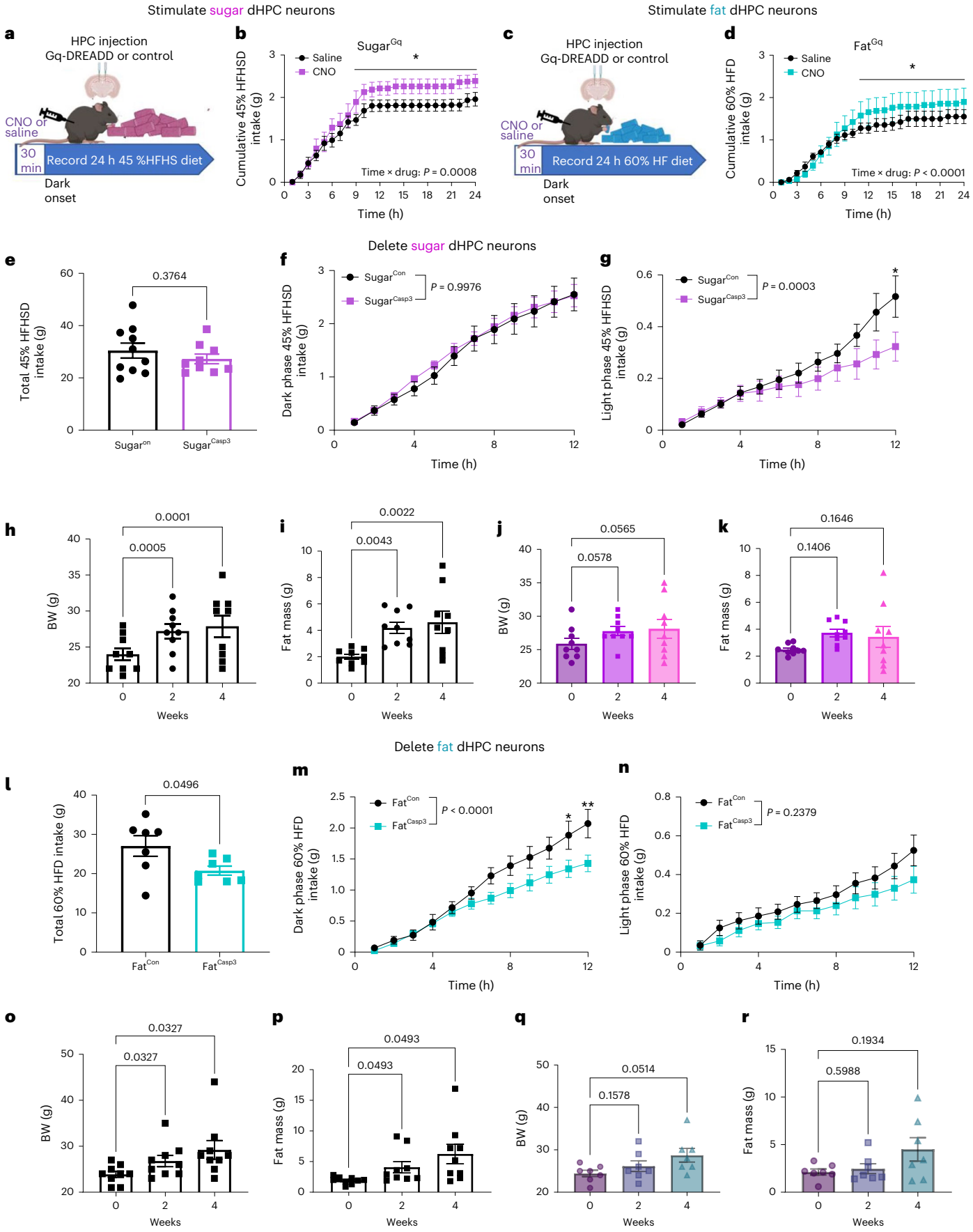

both of which promote food intake[36,37]. In humans, an orexigenic hippocampal circuit has recently been discovered that is strengthened in obesity[40]. Circuits have been identified that connect HPC neurons with brain regions associated with motivated behavior[23,45,82–88], but these have for the most part not been linked with increased food intake. An exception is a circuit from the vHPC to lateral hypothalamus, which is necessary to mediate endogenous ghrelin's orexigenic effect in meal entrainment[89]. Whether ghrelin-receptor-expressing vHPC neurons are an orexigenic population, or whether ghrelin inhibits an anorexigenic population, remains to be determined. This study identifies two previously unknown orexigenic populations in the dHPC.

We demonstrate a pivotal role for both dHPC neuronal populations in regulating the preference and intake of orally consumed solutions of isolated nutrients. Deleting nutrient-responsive dHPC neurons decreases consumption, whereas stimulation increases intake in a nutrient-specific manner. Specifically, dHPC^{Fat} neurons influence the quantity of fat solutions that animals consume, whereas dHPC^{Sugar} neurons exclusively govern sugar preference. These findings extend to complex diets, with dHPC^{Sugar} neurons impacting the number of HFHS diet meals consumed in the light phase, and dHPC^{Fat} neurons influencing the high-fat-diet meal size in the dark phase. Our findings reveal a previously unrecognized level of sophistication in hippocampal control of food intake, demonstrating that the dHPC is exquisitely attuned to the specific macronutrient composition of a meal.

Although the hippocampus has been implicated in hunger and satiety signaling[12,24–26], our study provides the first evidence for specific neuronal ensembles within the dHPC that directly encode post-ingestive nutrient signals. We demonstrate a causal role for the vagus nerve in conveying these signals to the brain. Our findings extend previous findings on vagal–hippocampal interactions, including vagal-mediated HPC neurogenesis[90–92], synaptic function[93,94], and hippocampal-dependent behavioral outcomes[47,48]. However, the incomplete blockade of dHPC activation following vagotomy suggests that additional pathways, such as gut hormone signaling[95–99] and/or spinal afferents, are involved. Although emerging evidence implicates spinal afferents innervating the intestine in glucose sensing and metabolism[100–102], a spinal–HPC circuit remains unidentified, and the role of spinal afferents in transmitting nutrient information beyond glucose to the brain remains to be established. Irrespective, our work fills a critical gap in knowledge by identifying fat and sugar as key physiological stimuli driving the activation of this gut–hippocampal circuit. These findings provide a mechanistic framework for understanding how the brain processes nutrient-specific information to influence food intake.

Explaining separate fat and sugar signaling mechanisms

An intriguing question that emerges from these findings is: why do distinct HPC neurons respond separately when activated by different post-ingestive stimuli? In the natural world, foods are rarely composed of a combination of both fat and sugar, potentially exerting selective evolutionary pressures that favored the development of separate biological systems for encoding distinct memories for either fat-rich or sugar-rich foods. Several studies have demonstrated that individuals exhibit more accurate spatial memory for the locations of high-calorie foods[103–105], hinting at the presence of memory systems finely tuned for efficiently locating and recalling nutritionally valuable food sources. These separate memory systems likely necessitate the ability to remember specific contextual cues associated with these different food types. We suggest that the formation of separate HPC neurons dedicated to either fat and sugar preference and appetitive memory might occur through one of two non-mutually-exclusive mechanisms.

Firstly, ingested fats and sugars might activate separate, parallel gut–brain circuits. Prior work from our lab provides evidence that fats and sugars are sensed by two separate populations of vagal sensory neurons[46]. Notably, the deletion of these vagal populations was shown to impair learned preferences in a nutrient-specific manner[46]. Furthermore, segregated cellular responses to fats or sugars in central reward circuits downstream of vagal sensory neurons were observed[46], suggesting that there are separate hardwired signaling mechanisms for rewards to different nutrients. In support of this possible mechanism, we found that stimulation of nutrient-specific vagal sensory neurons increases neuronal activity in the dHPC.

A second mechanism that could enable fat and sugar to activate separate dHPC populations is pattern separation. The DG in the HPC has a pivotal role in the process of pattern separation[106–109], a fundamental computation that allows neural circuits to distinguish between similar input activity patterns and transform them into distinct output patterns[110,111]. This mechanism is crucial for avoiding the confusion of memories associated with similar experiences. Pattern separation has been well-established in rodent studies[112–117] and is supported by human studies[118,119], in which the DG's large number of neurons and sparse coding contribute to the decorrelation of input signals before reaching CA3 (refs. 111,120). Lesions to the DG result in novelty-detection impairments following exposure to new spatial environments[121], highlighting its importance in reducing interference from previous experiences. We observe enrichment of DG activity in the dHPC in response to post-ingestive fat or sugar, which aligns with the possible role of the DG for discriminating contexts associated with appetitive compared with non-food related stimuli, but also encoding post-ingestive fat and sugar as dissimilar, non-overlapping memory representations.

Identification of an appetitive engram for sugar

Neurons in the HPC play a pivotal role in transforming new experiences into lasting memories that shape future behaviors. Immediate early genes (IEGs), like Fos, are transiently expressed in specific HPC neuron populations following learned experiences[122–124]. Reactivation of neurons on the basis of IEG activity is essential for memory retrieval[125], whereas inhibition of these ensembles impairs memory recall[126], underscoring the critical role of IEGs in consolidating and recalling specific memories. The use of activity-dependent expression of reporters therefore provides a framework for exploring engram ensemble.

The term 'engram,' first introduced by Richard Semon, describes a memory representation in the brain[127]. Since its introduction, efforts have focused on identifying these engrams on the basis of the ability to observe, erase, and artificially express them[128]. During memory formation, specific neuronal populations that constitute engram ensembles become activated and undergo cellular changes[129,130]. Inhibiting these changes impairs memory[126], and reactivation of these ensembles enable memory retrieval[125]. Although substantial progress has been made in understanding memory and engrams, particularly in the context of aversive and social interactions[125,131,132], an engram associated with appetitive memory has not been defined, despite evidence that memory for food is highly conserved across species from insects to humans[133–137].

Using the Fos^{TRAP} mouse model, we tagged neurons expressing Fos to target ensembles linked to appetitive stimuli. We found that a sparse network of Fos-expressing neurons in the dHPC responds to fat and sugar, encoding appetitive memory. This activation meets the first criterion for identifying a memory trace. Selectively deleting sugar-responsive or fat-responsive neurons reduced nutrient-specific memory expression, fulfilling the second criteria. Notably, deleting the neurons tagged in response to sugar impaired the contextual memory for sugar, demonstrating that different hippocampal engrams function separately[138]. Therefore, the sugar engram does not broadly disrupt memory retrieval, even of other appetitive memories.

Chemogenetic stimulation of sugar-responsive dHPC neurons during testing enhanced performance in a spatial memory task related to sugar, indicating that these neurons are sufficient for memory recall. By contrast, stimulating fat-responsive neurons did not improve fat-location memory performance. Moreover, ablating sugar-responsive neurons did not affect the initial learning of a

sugar-associated flavor preference, but did lead to a rapid decline in memory for this preference, underscoring the role of these neurons in memory expression after conditioning. Taken together, these data provide evidence of a sugar engram and demonstrate that dHPC populations for fat and sugar are distinct.

We also provide the first direct evidence that impaired memory for food location reduces food intake. Mice lacking sugar-responsive neurons consumed less sugar and had fewer meals of a sugar-rich diet during the light phase, suggesting a memory-based mechanism underlying sugar consumption. This aligns with the concept that remembering a food's location increases the likelihood of eating it, while forgetting reduces intake, as seen in people with Alzheimer's disease who experience reduced food intake owing to memory impairments[139,140].

In a separate set of experiments, we attempted to address the nature of the interrelationship between short-term memory (STM) and long-term memory (LTM). The debate whether these processes are distinct or part of a unified memory system is ongoing, with some research suggesting that STM is an active component of LTM[141–145] or part of a single system[146–151]. Recent neuroimaging research has leaned towards the idea of a unified memory system[149,152–158], although it might be difficult to parse out the overlapping features of STM and LTM that include encoding, retention, and recall. Our findings suggest that separate neural populations are involved in short-term working memory and long-term episodic memory, as deletion of sugar-responsive neurons in the dHPC impaired episodic memory without impacting performance in a task of working memory. Together, these results reveal a sugar-specific engram in the dHPC, show distinct neuron populations encoding fat and sugar memories, and underscore the role of food location memory in regulating intake and behavior, while also contributing to the broader understanding of memory systems.

The hedonic hippocampus

The precise role of the hippocampus in motivated behaviors, particularly in the context of reward seeking, remains controversial[33,159–162]. Our findings provide important insights by identifying a specific subset of hippocampal neurons crucial for motivation and learning related to fat rewards. These fat-responsive dHPC neurons are involved in assigning incentive salience to fat-related cues and facilitating Pavlovian conditioning, demonstrating a specialized role for the hippocampus in processing macronutrient-specific information. Notably, the effects of these neurons are specifically tied to food-related contexts, suggesting a more circumscribed function than that of general reward-processing systems. Intriguingly, sugar-responsive neurons had no effect on motivation to work for a sugar reward or formation of conditioned preference associated with sugar, aligning with previous studies indicating that hippocampal lesions do not impact sugar conditioning[70]. These results further underscore the different functions of fat and sugar dHPC neurons.

Our results align with previous work identifying hippocampal neurons that encode reward location across contingencies and environments[62]. These neurons are thought to be involved in the process of encoding and retrieving memories related to rewards, regardless of the context in which the reward was experienced. Our data suggest a possible role for these neurons in mapping the site of a reward and/or increasing the motivation to access the reward.

Conclusion

The HPC is a brain region recognized for its role in learning and memory, but our findings reveal a more complex role in controlling food intake. The HPC acts as a critical nexus integrating sensory, motivational, and mnemonic processes to guide feeding decisions. We demonstrate that sugar-responsive dHPC neurons are part of an appetitive engram that encodes sugar location memory that can be erased or artificially activated. Conversely, fat-responsive dHPC neurons promote motivation and strengthen cue associations for post-ingestive fat. These neurons therefore have separate functions in creating an internal model that maps the environmental availability and locations of high-calorie foods (sugar neurons) and modulates the internal drive to obtain them (fat neurons). In our current food environment, there is the potential for devastating impact of these orexigenic neurons to exacerbate cue-induced consumption of obesogenic foods rich in fat and sugar. By elucidating the neural mechanisms underlying nutrient-specific consumption, our findings provide a foundation for developing strategies to counteract the obesogenic environment.

Methods

Animals and housing

All animal procedures followed ethical guidelines, and all protocols were approved by the Institutional Animal Care and Use Committee (IACUC) at the University of Florida (protocol no. 202110305) and Monell Chemical Senses Center (protocol nos. 1187 and 1190). Adult mice (6–20 weeks; males and females; C57BL/6J background) were used and maintained on a reverse 12-h light–dark circle. Animals were purchased and bred in house. Strain details and number of animals in each group are as follows. C57BL/6J wild type: $n = 84$; 42 male, 42 female. Fos Cre tdTomato: $n = 116$; 58 male, 58 female. These mice were generated by crossing Jackson Laboratory B6.129(Cg)-Fos$^{tm1.1(cre/ERT2)Luo}$/J (JAX stock no.021882) and Ai14 (B6.Cg-Gt(ROSA)26Sor$^{tm14(CAG-tdTomato)Hze}$/J, JAX stock no.007914). Animals were single housed at 22 °C, 40–60% humidity, with ad libitum access to standard rodent chow (3.1 kcal g^{-1}, Teklad 2018, Envigo) or HFHS diet (45% calories from fat; 4.7 kcal g^{-1}, Research Diets D12451) or HF diet (60% calories from fat; 5.2 kcal g^{-1}; Research Diets D12492), unless stated otherwise. Prior to experiments, animals were habituated to experimental conditions for 2–3 days.

TRAP protocol

As previously described[46], animals were fasted for 6 h prior to IG infusion. Thirty minutes before onset of the dark phase, mice received an IG infusion of sugar solution (15%, wt/vol, sucrose) or fat solution (6.8%, vol/vol, Microlipid) (500 µl, 100 µl min^{-1}) in their home cage, on the basis of their assigned group. 4-OHT (30 mg kg^{-1}, i.p., MilliporeSigma) was injected 3 h after the stimulus, and standard chow was returned to animals' home cage 3 h after 4-OHT injection.

Surgeries

IG catheter implantation. IG catheters were made from 6 cm silicon tubing (.047" OD × .024" ID, SIL047, Braintree Scientific) composed of 6 beads of silicon glue (no. 31003, Marineland) and a Pinport (Instech Labs) for infusions. Analgesics buprenorphine XR (1 mg kg^{-1}) and carprofen (5 mg kg^{-1}) were injected (subcutaneously (s.c.)) 20 minutes prior to the surgery. Once animals had been anesthetized, a midline incision was made with a scalpel into the abdomen, and hemostats were used to blunt dissect the skin layer away from the muscle layer to allow the catheter to be pulled between the abdominal incision site and the back of neck incision site. The stomach was exteriorized using a blunt forcep and a 4-mm purse suture was then placed at the junction of the greater curvature and fundus. Fine tip forceps were used to puncture the center of the purse suture, and the end of the IG catheter was inserted into the stomach. The purse suture was then tightened and tied around the catheter. Next, a puncture hole was made in the left lateral abdominal wall using fine tip forceps, and the catheter was pulled through and secured using 5-0 absorbable suture. The muscle layer of the abdominal incision site was then sutured, and the open end of the catheter was pulled through to the back of the neck through a hole made in the middle of the shoulder blade. A 22-gauge Pinport was anchored in the tubing using superglue and once the patency of the catheter was confirmed through flushing with sterile saline, the catheter was secured with a purse suture around the hole in the back. Finally, the skin of the abdomen was closed with sterilized suture clips. For recovery, animals were fed with moistened chow in their home cage and were administered carprofen for 2 days after the surgery.

Vagotomy. Surgeries were performed aseptically following the IACUC Guidelines for Rodent survival surgery. Mice were anesthetized by inhalation of a continuous flow of 1.5–2% isoflurane. The pedal reflex test was performed before surgery to ensure that each mouse had reached an appropriate level of anesthesia. Mice were placed on a sterile drape warmed by a heating pad. Fur was shaved from the abdomen before cleansing with three exchanges of ethanol and betadine. Sterile surgical equipment was used to create a 2–4 cm midline laparotomy. The small intestine and colon were externalized and placed on sterile gauze moistened with sterile 0.9% NaCl saline. The subdiaphragmatic vagus nerve was visualized by gentle retraction of the liver and stomach. Complete subdiaphragmatic vagotomy was performed by cutting the left and right branches of the vagus directly caudal of the diaphragm using spring scissors. Sham animals had their subdiaphragmatic vagus nerve visualized, but it was not tampered with. The internal organs were repositioned and the incision site was covered with sterile gauze moistened with 0.9% NaCl saline until intestinal infusions.

Following the vagotomy, a silicone tubing was inserted via a small opening in the stomach wall, into the proximal section of the duodenal lumen. The duodenum received a 5-minute infusion of either sucrose (15%, wt/vol or fat (6.8%, vol/vol) solution (500 µl, 100 µl minute^{-1}). Post-stimulation, incisions were sutured, and the mice were allowed to recover on a heating pad until they voluntarily moved to the unheated section of the cage. After 90 minutes, the mice were perfused and their brains were collected, post-fixed in 4% PFA for 24 h and kept at 4 °C in a 30% sucrose in PBS solution until processing.

Nodose ganglia injection

The animals received a subcutaneous injection of carprofen (5 mg kg^{-1}; Henry Schein) 10 minutes before surgery. Anesthesia was induced with 1.5–2.5% isoflurane, and a 2-cm midline incision was made on the ventral aspect of the neck. After retracting the salivary glands and lymph nodes, the vagus nerve was carefully separated from the carotid artery using fine-tip forceps. The NG was exposed by retracting the surrounding muscle and dissecting the connective tissue. A micromanipulator equipped with a glass pipette (30-µm tip diameter, beveled at a 45-degree angle) was used to position and puncture sheath of the NG. A Picospritzer III injector (Parker Hannifin) was used to control the injection speed and volume (total volume, 0.25 µl) directly into the NG, with the animals receiving either a control virus (pAAV9-EF1a-DIO-EYFP, Addgene 27056) or a Cre-dependent ChR2 virus (pAAV9-Ef1a-double floxed-hChR2(H134R)-EYFP-WPRE-HGHpA, Addgene 20298). The incision site was then closed using 5-0 sutures. Animals were fed with moistened chow, and a post-operative analgesic was administered 24 h after the surgery. Two weeks after the NG injections, a GI catheter was implanted, and animals were then trapped with either sugar or fat. Optogenetic stimulation was applied to the NG bilaterally (30 s at 5 mW intensity per side), and the animals were perfused 90 minutes later. Brains were then collected for cFos staining, and NG were collected to validate ChR2 expression.

Stereotaxic viral injections

Mice were anaesthetized with 1.5–2% isoflurane and were injected with carprofen analgesia (5 mg kg^{-1}, s.c.) before bilateral injection in the dorsal hippocampus (dHPC). Core temperature was maintained using a homeothermic monitoring system, and the absence of pedal reflex was utilized as a standard for appropriate depth of anesthesia. Animals were restrained in a stereotaxic frame (World Precision Instruments), and their skulls were secured by positioning the bilateral ear crossbars into auditory meatus. A 2- to 3-mm incision was made in the midline of the scalp using a scalpel, and the sagittal suture, bregma, and lambda of the skull were then exposed. With the bregma serving as an anatomical landmark, a dental drill was used to penetrate the skull above the target brain area. For dHPC viral injections, a Hamilton neuros syringe filled with a viral construct was lowered to the injection site in the dHPC (anteroposterior (AP), −1.8 mm; mediolateral (ML), ± 0.4 mm; dorsoventral (DV), −2.1 mm). The viral construct (0.2 µl per side, 0.1 µl minutes^{-1}) was injected through a stereotaxic injector pump (Harvard Apparatus), and the needle remained in place for a further 10 minutes to minimize the backflow of solution out of the injection site. The needle was removed slowly after the injection, and a 5-0 absorbable suture was used to close the skin. pAAV5-flex-taCasp3-TEVp was a gift from N. Shah and J. Wells (Addgene no. 45580)[58]; pAAV9-EF1a-DIO-hM3D(Gq)-mCherry was a gift from B. Roth (Addgene no. 44361); and pAAV-EF1a-DIO-EYFP was a gift from B. Roth (Addgene no. 27056, both AAV5 and AAV9 serotypes were used)[163].

Behavioral tests

Food restriction. For all memory and motivation tasks involving food, animals were maintained at 85–90% of their original body weight by food restriction. In brief, for weight maintenance, the animals' body weight was recorded every 24 h, and they were fed with a set amount of food calculated on the basis of the loss of their original body weight. Animals were restricted from food 6 h before the task and were not refed until 2 h after the end of the task to prevent interference from food consumed outside of the task. If any mouse weighed less than 85% of their starting body weight, they were fed 2.5 g plus the excess weight loss until they reached 85% of their starting body weight. Ad libitum water access was provided in the home cage.

Food intake measurement. Food intake measurement and meal-pattern analysis were performed using the BioDAQ episodic Food Intake Monitor (BioDAQ, Research Diets). Previously validated meal criteria were used for food intake analysis (minimal meal size, 0.02 g; maximum inter-meal interval, 300 s)[164]. Animals were single-housed, acclimated to the BioDAQ cages, and fed ad libitum with chow for at least 3 days. For the caspase ablation study involving obesogenic diet intake measurement, animals were switched to their respective diets following the acclimation period. Their intake was then continuously monitored using a BioDAQ system for at least 10 days. For the Gq stimulation study, animals were maintained on an obesogenic diet for 5 days and trained to receive i.p. injection. On the experimental day, the mice were injected with either saline or CNO 30 minutes before the dark phase, and food intake was measured over the next 24 h. Meal parameters including meal size, the number of meals (meal frequency), meal duration, and inter-meal interval were calculated using the BioDAQ Monitoring Software.

Body-composition analysis

Whole-body-composition analysis was performed using EchoMRI before and after 2 and 4 weeks of obesogenic diet consumption, depending on the animals' assigned group. In brief, following daily calibration of the EchoMRI device, the animals were gently placed in a plastic tube designed for EchoMRI analysis. The tube was then inserted into the EchoMRI, and fat mass was measured.

Behavioral experiments

Measurement of nutrient solution consumption and flavor-nutrient conditioning tests were conducted in mouse behavioral chambers enclosed in a ventilated and sound-attenuating cubicle (Med Associates). Each chamber was equipped with slots for sipper tubing, equipped with contact lickometers with 10-ms resolution (Med Associates) that were used to detect licking. Licking and behavioral data were collected using the proprietary MedPC-V Software Suite. All memory tests, except for the nutrient-driven Barnes Maze task, were conducted in open field apparatus (41 × 41 cm; 30 cm height). The foraging-related Barnes maze task[47] involved an elevated white circular Barnes maze (diameter, 92 cm; height, 95 cm) with 16 holes (diameter, 5 cm), evenly spaced around the outer edge of the table's circumference. The holes were covered with Petri dishes, and visuospatial cues were placed on

each of the walls surrounding the table. XT Behavior Tracking Software (Noldus Information Technology; version 17) was used for behavioral analysis. The experimental apparatus was first outlined by defining an arena in the software. Specific zones were then created and defined to encompass the objects in the arena. Animal tracking was conducted on the basis of head or body position.

Measurement of nutrient solution consumption

Food-restricted mice were habituated and trained in these operant chambers with saccharin (0.2%, wt/vol) for 1 h per day for at least 3 days, or until their number of total licks reached at least 1,000 licks h^{-1}. The bottle containing saccharin was placed in a different slot each day to avoid side preference. For caspase ablation studies, once animals were fully trained, they underwent consumption tests for either sucrose solution (15%, wt/vol) or isocaloric fat solution (6.8%, vol/vol) in a randomized order to minimize the influence of systematic contrast effects. Next, during consumption preference tests, one bottle with sucrose solution was placed on one side, and another bottle with isocaloric fat solution was placed on the other side. All the tests were conducted for 30 min day^{-1} for 3 days, and the number of licks was recorded. In one batch of animals, the bottle location was swapped every 10 minutes. For chemogenetic manipulation, baseline sucrose or fat consumption was assessed 20 minutes after saline injection, until the animals consumed similar amounts (±10%) for 3 consecutive days. On the day of the experiment, sucrose or fat consumption was measured 20 minutes following the administration of CNO (diluted in saline, 3 mg kg^{-1}, Enzo Life Sciences).

Brief-access taste acceptance test

Brief-exposure taste acceptance was assessed using MS160-Mouse gustometers manufactured by DiLog Instruments (now manufactured by Med Associates) using proprietary Davis Rig software. Each gustometer consists of a test chamber (14.5 cm × 15 cm × 15 cm) with a motorized shutter that controls access to a taste solution. Bottles of taste solution are mounted on a rack that is precisely positioned by a stepper motor so that any one of eight different taste solutions can be presented to the mouse. The drinking spout of each bottle is part of a high-frequency alternating current contact circuit, so that each lick the mouse makes is detected and recorded. To train the mice to sample taste solutions (sucrose, 0–30%, wt/vol; fat, 0–13.4%, vol/vol), they were first deprived of water for 22.5 h and then placed into a gustometer with its shutter open. During the first training session, each mouse had continuous access to water for 30 minutes. It was then returned to its home cage and given water for 1 h. During the following 2 days, this procedure was repeated, except the shutter allowing access to water was closed 5 seconds after each time the mouse began to lick and was reopened after a 7.5-second interval. After 20 minutes, the mouse was returned to its home cage and given water for 1 h. By the second test using these procedures, all mice had learned to obtain water during the 5-seconds access periods.

Flavor nutrient conditioning test

To test whether ablation of nutrient-responsive HPC neurons affects specific nutrient–flavor association, a two-bottle preference test was performed. Once animals were trained to lick saccharin, as described previously, a pretest was performed in which mice were given 1 h access to two novel Kool-Aid flavored solutions (cherry or grape, 0.05%, wt/vol) in saccharin (0.025%, wt/vol). To avoid development of side preference, sipper bottle positions were switched after 30 minutes. Subsequently, animals underwent a 1-h conditioning session each day for 6 days, during which the less preferred flavor defined in the pretest was paired with IG infusions of isocaloric nutrients (CS+; 6.8% fat or 15% sucrose), and the preferred flavor was paired with IG infusions of saline (CS−). Specifically, during conditioning sessions, IG infusions of either nutrients or saline delivered by a syringe pump (20 µl per lick, 600 µl $minute^{-1}$) were triggered by detection of the first lick, and additional licks detected within 6 seconds had no programmed consequences. Upon completion of these conditioning sessions, mice underwent a post-test identical to the pretest without IG infusions. The number of licks for the nutrient-paired flavor during the pre- and post-tests was used to calculate flavor preference ratios (CS+ licks / total licks) before and after conditioning. For $dHPC^{Sugar}$ mice, an additional post-test was performed 2 days after the initial post-test to assess memory of the post-ingestive sucrose-conditioned flavor. To evaluate whether the impaired fat conditioning in the caspase-treated $dHPC^{Fat}$ group was due to fewer fat infusions or impaired learning, the pair-fed group was limited to 22 fat infusions, matching the number received by the $dHPC^{Fat}$ ablation group.

Progressive ratio licking test

To assess whether nutrient-responsive dHPC neurons are important for nutrient-specific motivation, a progressive ratio (PR) operant licking test[69] was performed. Food-restricted mice were initially trained to lick an active sipper spout to receive 15% sucrose or isocaloric fat solution through tubing mounted in a syringe pump (1 µl per lick, 600 µl $minute^{-1}$) under fixed ratio 1 (FR1) schedule (1 h day^{-1} for 3 days). After reaching >80% discrimination for the active sipper over the inactive sipper, the schedule was increased to FR5 for an additional 2 days. Tests under the PR schedule were then performed, and failure to lick the active sipper in any 10-minute period resulted in termination of the session (1 h per session). For chemogenetic experiments, on PR test days, mice received either saline or CNO (i.p; 3 mg kg^{-1}) 20 minutes prior to entering the operant chamber in a counterbalanced design. The number of licks was recorded, and the breakpoint of reinforcement was calculated to quantify an animal's willingness to work for a nutrient solution.

Nutrient-driven food location memory test

To assess whether nutrient-responsive dHPC neurons are necessary for food location reference memory, a modified nutrient-driven food cup task[23,165] was conducted. Food-restricted mice were habituated in an open-field apparatus with visual cues, as described previously, for 5 minutes. The next day, a pretest was performed in which animals were allowed to explore the same arena containing two empty Petri dishes placed in opposite corners for 5 minutes, and the baseline preference for two quadrants was determined. Twenty-four hours later, animals underwent conditioning sessions (3 × 5-minute sessions) in which the less-preferred quadrant was paired with a Petri dish containing drops of nutrient solution (CS+, 20 × 10 µl drops per session) and the preferred quadrant was paired with a Petri dish containing drops of water (CS−, 20 × 10 µl drops per session). One hour or 24 h after the last conditioning session, a post-test identical to the pretest was conducted in which both Petri dishes were available with no stimuli. The time spent exploring each Petri dish was recorded across the whole experiment, and the discrimination index was calculated as the time spent exploring CS+ / total exploration time, to assess animals' memory performance.

Nutrient-driven food location memory test with chemogenetic manipulation

To evaluate the role of nutrient-responsive dHPC neurons in context-dependent spatial memory for specific nutrients, a modified food location memory task was conducted with chemogenetic manipulation using CNO. Mice expressing hM3Dq or control virus in dHPC neurons trapped with IG infusion of sucrose (15% wt/vol) or fat (6.8% vol/vol) were habituated to two novel environments (context A and context B) with two clean Petri dishes on opposing quadrants. During a 3-day training phase, fat or sugar rewards (CS+, 20 × 10 µl drops per Petri dish) or water (CS−) were placed in opposite quadrants within each context, with the specific locations of the rewards and water different between contexts. Mice received saline injections 20 min before each training

session for 10 min, and were exposed to one context in the morning and the other in the afternoon. A 24-h retention test with empty Petri dishes assessed initial memory performance in each context. Seven days later, the experiment was repeated, but mice received CNO (3 mg kg^{-1}) 20 min before being placed in either the context paired with their trapped nutrient or the opposite context. Time spent exploring each Petri dish was recorded, and a discrimination index was calculated to evaluate memory performance.

Nutrient-driven Barnes maze test

To evaluate the effect of nutrient-responsive dHPC neurons on food-related spatial working memory, a modified Barnes maze test was performed[47]. The holes were covered on the maze and 16 Petri dishes were placed evenly distributed around the edge. Food-restricted mice were first allowed to explore the Barnes maze apparatus for 5 minutes. The next day, animals were trained to use spatial cues to locate the single Petri dish containing sucrose (15% wt/vol) or isocaloric fat (6.8% vol/vol). All other Petri dishes contained water. Each animal received two trials per day for three training days with 2-minute intertrial interval. Between trials, the maze was cleaned using 70% ethanol to avoid any confounding odor effect. Importantly, the target dish remained in a consistent position in both trials conducted on each training day, but was relocated to a new position at the beginning of the initial trial on each subsequent training day. The number of incorrect investigations were recorded, and the difference in the number of errors between trial 2 and trial 1 on an individual training day was calculated to determine whether animals improved their appetitive spatial working memory performance.

Novel object in context test

To assess the specificity of nutrient-responsive dHPC neurons in modulating non-food related memory, an HPC-dependent novel object in context test (NOIC) test[166] was performed. Animals underwent 10 minutes of habituation to two distinct environments on separate days (context A, an opaque box with black stripes; context B, an opaque box with no stripes). On day three, half of the animals were placed in context A for 10 minutes with two identical Lego blocks (object 1) positioned on opposite corners, and the other half were first placed in context B for 10 minutes with a different set of identical Lego blocks (object 2) placed in opposite corners. Animals were then switched and trained in the other context for another 10 minutes, spending 1–3 minutes in their home cage between contexts. Twenty-four hours later, the NOIC recognition test was conducted by placing animals in their last trained context (familiar context) for 10 minutes, with one object familiar to the context and one novel object belonging to the other context. The amount of time spent exploring the objects (t_{novel} and $t_{familiar}$) was recorded, and a discrimination index was calculated as t_{novel} / (t_{novel} + $t_{familiar}$) to assess memory performance. Seventy percent ethanol was used to clean all objects and contexts between tests.

Conditioned place preference test

A CPP paradigm was performed to assess whether activating nutrient-responsive dHPC neurons induced nutrient-specific motivation. In a pretest, animals were exposed for 15 minutes to the CPP apparatus (Med Associates) containing two distinct chambers with different floors and walls to establish baseline preferences. Subsequently, a 4-day conditioning phase was implemented, pairing the less preferred chamber with CNO injections (3 mg kg^{-1}, i.p.) and the other with saline. Animals were alternated between chambers daily, with CNO or saline administered 20 minutes prior to chamber entry. A 15-minute post-conditioning test assessed chamber preference in the absence of injections. The amount of time spent in each chamber was recorded using video tracking software, and a preference index was calculated as time spent exploring the CNO-paired chamber / total exploration time.

Histology

Transcardial perfusion was performed in deeply anesthetized animals with PBS, followed by 4% PFA. Following perfusion, brains were collected and left in 4% paraformaldehyde for 24 h and then transferred to a 30% sucrose solution containing 0.1% sodium azide for at least 72 h before further processing. In some experiments, nodose ganglia were collected and left in 4% PFA for 1 h and transferred to 30% sucrose/sodium azide solution for 24 h.

Tissue processing and storage

Slicing. Whole brains were frozen and embedded in optimal cutting temperature compound. A Leica frozen microtome (CM 3050 S, Leica Biosystems) was used to section the tissue into 3 series at a thickness of 35 µm per section for cFos staining and 20 µm per section for RNAscope. Slices were stored in cryoprotectant at −80 °C for immunohistochemistry.

Immunohistochemistry: Fos. The tissue was removed from cryoprotectant and rinsed in PBS 3 times (10 minutes each time) at room temperature. Subsequently, tissue was incubated for 30 minutes in a blocking buffer consisting of permeabilizing agent (244.5 ml of PBS, 5 ml of serum, 0.5 ml of Triton X-100, 0.25 g of BSA) and 20% normal donkey serum at 37 °C to prevent non-specific antibody binding. Tissue was then incubated overnight in permeabilizing agent containing a rabbit anti-cFos primary antibody (1:1,000, Cell Signaling, clone 9F6) at 4 °C. On the following day, the tissue was rinsed in PBS 3 times (20 minutes each time) at room temperature, followed by incubation in PA containing a Alexa Fluor 647-conjugated donkey anti-rabbit-IgG secondary antibody (1:500, Abcam). Tissue was then rinsed in PBS 3 times (1 h each time), mounted on slides, coverslipped with Prolong Diamond Antifade Mountant (Invitrogen), and stored at −20 °C until imaging and analysis.

RNAscope. To characterize nutrient-responsive HPC neurons, we used RNAscope for single-molecule fluorescence in situ hybridization using a fluorescent multiplex kit (Advanced Cell Diagnostics) on 20-µm-thick HPC sections. Tissue sections were first placed in the HybEZ II Oven for 30 minutes and then post-fixed in prechilled 4% PFA for 15 minutes. After fixation, the sections were subjected to sequential ethanol washes (5 minutes each in 50%, 70%, and 100% ethanol, with an additional 100% ethanol wash). Once fully dried, RNAscope hydrogen peroxide solution was applied to the sections and incubated at room temperature for 10 minutes. Following several washes in distilled water, the target retrieval was performed using a steamer. Protein digestion was then carried out with protease III at 40 °C for 30 minutes, followed by two rinses in distilled water. An Slc32a1 (319191-C2) or Slc17a7 (501101-C2) probe was then applied to the slides and incubated in a humidified oven at 40 °C for 2 h. The slides were rinsed twice with RNAscope wash buffer, and colorimetric reactions were performed according to the standardized protocol provided with the kit (OPAL, Akoya Biosciences). After the final wash, tissue sections were incubated with DAPI (from the RNAscope kit) for 30 seconds and then covered with FluoroGel.

Imaging

The HPC and PVH were identified using a mouse brain atlas[167]. During image acquisition, the experimenter was blinded to the treatment condition. Images of each region of interest (ROI) were acquired with a Keyence BZ-X800 microscope using a ×10 objective. Images were stitched using the BZ-X800 analyzer with the correct-shading function. To quantify the number of positive cells, including trapped cells, Fos^+ cells, and their colocalization, we used a semi-automated approach using NIS Elements AR Analysis software (version 5.11.01) and at least three sections per region per mouse were quantified. For dorsal HPC (bregma, −1.8 mm ± 0.4 mm) and ventral HPC (bregma,

−3 mm ± 0.2 mm) slice quantification, an ROI encompassing the HPC was drawn for both hemispheres. The cells were automatically identified and counted using the Bright Spot Detection function, with diameter and contrast filters were applied to ensure precise selection. The same filters were applied to all images and adjusted mildly between mice. Overlap between trapped cells and Fos$^+$ cells were calculated as the number of double$^+$ cells (TRAP$^+$ and Fos$^+$) in all Fos$^+$ cells. Final data were represented as the number of cells per section averaged from all the slices in the area of interest in one hemisphere. For PVH slices (bregma, −1 mm ± 0.2 mm) quantification, a similar method was employed. However, the final data reflect the total number of cells within the entire ROI, rather than cell counts in one hemisphere.

For the NG image, whole NG samples were imaged with a ×16 objective using a 2-photon microscope (Bruker) taking optical *z*-stacks every 20 µm with proprietary Prairie View v5.7 software. The final figure displays a single section from the *z*-stack for each channel.

Data analysis

No statistical methods were used to pre-determine sample sizes, but our sample sizes are similar to those reported in previous publications[23,46]. All experiments were performed in pseudo-random counterbalanced design with all animals receiving each treatment. All data were analyzed by investigators blinded to the treatment conditions, but investigators were not blinded to group allocations. Only mice with AAV-mediated protein expression confined to the injection target region (hippocampus) were included in the final analysis. Statistical analyses are described for each figure and were performed using GraphPad Prism software, version 10. Two-tailed unpaired Student's *t*-tests were used to compare two groups; two-tailed paired Student's *t*-tests were used to compare two treatments or tests in the same animal. One-way ANOVA, with or without repeated measures, was used to compare three groups; two-way ANOVA, with or without repeated measures, was used to compare more than one factor between groups. Data are presented as mean ± s.e.m., and statistical significance is declared at $P < 0.05$. The data met the assumptions of the statistical tests used. Normality and equal variances were formally tested.

Reporting summary

Further information on research design is available in the Nature Portfolio Reporting Summary linked to this article.

Data availability

There are no publicly available datasets for this manuscript. All data necessary to interpret, replicate, and build upon the methods or findings reported here are contained within the manuscript and supplemental information. All mouse lines, plasmids, and reagents used in this study have been previously published and/or are commercially available, and are detailed in the Reporting Summary. Further information and requests for resources and reagents should be directed to and will be fulfilled by G.d.L. Source data are provided with this paper.

References

1. Kanoski, S. E. & Boutelle, K. N. Food cue reactivity: neurobiological and behavioral underpinnings. *Rev. Endocr. Metab. Disord.* **23**, 683–696 (2022).
2. Petrovich, G. D., Ross, C. A., Gallagher, M. & Holland, P. C. Learned contextual cue potentiates eating in rats. *Physiol. Behav.* **90**, 362–367 (2007).
3. Killgore, W. D. et al. Cortico-limbic responsiveness to high-calorie food images predicts weight status among women. *Int. J. Obes.* **37**, 1435–1442 (2013).
4. Yokum, S., Ng, J. & Stice, E. Attentional bias to food images associated with elevated weight and future weight gain: an fMRI study. *Obesity* **19**, 1775–1783 (2011).
5. Demos, K. E., Heatherton, T. F. & Kelley, W. M. Individual differences in nucleus accumbens activity to food and sexual images predict weight gain and sexual behavior. *J. Neurosci.* **32**, 5549–5552 (2012).
6. Van der Laan, L. N., De Ridder, D. T. D., Viergever, M. A. & Smeets, P. A. M. Appearance matters: neural correlates of food choice and packaging aesthetics. *PLoS ONE* **7**, e41738 (2012).
7. Mehta, S. et al. Regional brain response to visual food cues is a marker of satiety that predicts food choice. *Am. J. Clin. Nutr.* **96**, 989–999 (2012).
8. O'Keefe, J. & Dostrovsky, J. The hippocampus as a spatial map. Preliminary evidence from unit activity in the freely-moving rat. *Brain Res.* **34**, 171–175 (1971).
9. Eichenbaum, H. Prefrontal–hippocampal interactions in episodic memory. *Nat. Rev. Neurosci.* **18**, 547–558 (2017).
10. Rolls, E. T. The mechanisms for pattern completion and pattern separation in the hippocampus. *Front. Syst. Neurosci.* **7**, 74 (2013).
11. Davidson, T. L. et al. Contributions of the hippocampus and medial prefrontal cortex to energy and body weight regulation. *Hippocampus* **19**, 235–252 (2009).
12. Kanoski, S. E. & Grill, H. J. Hippocampus contributions to food intake control: mnemonic, neuroanatomical, and endocrine mechanisms. *Biol. Psychiatry* **81**, 748–756 (2017).
13. Min, D. K., Tuor, U. I., Koopmans, H. S. & Chelikani, P. K. Changes in differential functional magnetic resonance signals in the rodent brain elicited by mixed-nutrient or protein-enriched meals. *Gastroenterology* **141**, 1832–1841 (2011).
14. Vanderwolf, C. H. Hippocampal activity, olfaction, and sniffing: an olfactory input to the dentate gyrus. *Brain Res.* **593**, 197–208 (1992).
15. Wood, E. R., Dudchenko, P. A. & Eichenbaum, H. The global record of memory in hippocampal neuronal activity. *Nature* **397**, 613–616 (1999).
16. Haase, L., Cerf-Ducastel, B. & Murphy, C. Cortical activation in response to pure taste stimuli during the physiological states of hunger and satiety. *Neuroimage* **44**, 1008–1021 (2009).
17. Spetter, M. S., Smeets, P. A. M., de Graaf, C. & Viergever, M. A. Representation of sweet and salty taste intensity in the brain. *Chem. Senses* **35**, 831–840 (2010).
18. Shapiro, M. L., Tanila, H. & Eichenbaum, H. Cues that hippocampal place cells encode: dynamic and hierarchical representation of local and distal stimuli. *Hippocampus* **7**, 624–642 (1997).
19. Moita, M. A., Rosis, S., Zhou, Y., LeDoux, J. E. & Blair, H. T. Hippocampal place cells acquire location-specific responses to the conditioned stimulus during auditory fear conditioning. *Neuron* **37**, 485–497 (2003).
20. Fried, I., MacDonald, K. A. & Wilson, C. L. Single neuron activity in human hippocampus and amygdala during recognition of faces and objects. *Neuron* **18**, 753–765 (1997).
21. King, B. M. et al. Hyperphagia and obesity in female rats with temporal lobe lesions. *Physiol. Behav.* **54**, 759–765 (1993).
22. Forloni, G., Fisone, G., Guaitani, A., Ladinsky, H. & Consolo, S. Role of the hippocampus in the sex-dependent regulation of eating behavior: studies with kainic acid. *Physiol. Behav.* **38**, 321–326 (1986).
23. Azevedo, E. P. et al. A role of Drd2 hippocampal neurons in context-dependent food intake. *Neuron* **102**, 873–886 (2019).
24. Hebben, N., Corkin, S., Eichenbaum, H. & Shedlack, K. Diminished ability to interpret and report internal states after bilateral medial temporal resection: case H.M. *Behav. Neurosci.* **99**, 1031–1039 (1985).
25. Rozin, P., Dow, S., Moscovitch, M. & Rajaram, S. What causes humans to begin and end a meal? A role for memory for what has been eaten, as evidenced by a study of multiple meal eating in amnesic patients. *Psychol. Sci.* **9**, 392–396 (1998).

26. Davidson, T. L. & Jarrard, L. A role for hippocampus in the utilization of hunger signals. *Behav. Neural Biol.* **59**, 167–171 (1993).
27. Hirsh, R. The hippocampus and contextual retrieval of information from memory: a theory. *Behav. Biol.* **12**, 421–444 (1974).
28. DelParigi, A. et al. Persistence of abnormal neural responses to a meal in postobese individuals. *Int. J. Obes. Relat. Metab. Disord.* **28**, 370–377 (2004).
29. Kanoski, S. E. & Davidson, T. L. Western diet consumption and cognitive impairment: links to hippocampal dysfunction and obesity. *Physiol. Behav.* **103**, 59–68 (2011).
30. Hannapel, R. et al. Postmeal optogenetic inhibition of dorsal or ventral hippocampal pyramidal neurons increases future intake. *eNeuro* **6**, ENEURO.0457-18.2018 (2019).
31. Henderson, Y. O., Smith, G. P. & Parent, M. B. Hippocampal neurons inhibit meal onset. *Hippocampus* **23**, 100–107 (2013).
32. Li, X. L. et al. Impairment of long-term potentiation and spatial memory in leptin receptor-deficient rodents. *Neuroscience* **113**, 607–615 (2002).
33. Schmelzeis, M. C. & Mittleman, G. The hippocampus and reward: effects of hippocampal lesions on progressive-ratio responding. *Behav. Neurosci.* **110**, 1049–1066 (1996).
34. Hsu, T. M. et al. Hippocampus ghrelin receptor signaling promotes socially-mediated learned food preference. *Neuropharmacology* **131**, 487–496 (2018).
35. Kanoski, S. E., Fortin, S. M., Ricks, K. M. & Grill, H. J. Ghrelin signaling in the ventral hippocampus stimulates learned and motivational aspects of feeding via PI3K–Akt signaling. *Biol. Psychiatry* **73**, 915–923 (2013).
36. Stoeckel, L. E. et al. Widespread reward-system activation in obese women in response to pictures of high-calorie foods. *Neuroimage* **41**, 636–647 (2008).
37. Connolly, L. et al. Differences in brain responses between lean and obese women to a sweetened drink. *Neurogastroenterol. Motil.* **25**, 579–e460 (2013).
38. Birch, L. L., McPhee, L., Sullivan, S. & Johnson, S. Conditioned meal initiation in young children. *Appetite* **13**, 105–113 (1989).
39. Cornell, C. E., Rodin, J. & Weingarten, H. Stimulus-induced eating when satiated. *Physiol. Behav.* **45**, 695–704 (1989).
40. Barbosa, D. A. N. et al. An orexigenic subnetwork within the human hippocampus. *Nature* **621**, 381–388 (2023).
41. Vanrobaeys, Y. et al. Mapping the spatial transcriptomic signature of the hippocampus during memory consolidation. *Nat. Commun.* **14**, 6100 (2023).
42. Lacar, B. et al. Nuclear RNA-seq of single neurons reveals molecular signatures of activation. *Nat. Commun.* **7**, 11022 (2016).
43. Grégoire, C.-A. et al. RNA-sequencing reveals unique transcriptional signatures of running and running-independent environmental enrichment in the adult mouse dentate gyrus. *Front. Mol. Neurosci.* **11**, 126 (2018).
44. Lee, A.-R., Kim, J.-H., Cho, E., Kim, M. & Park, M. Dorsal and ventral hippocampus differentiate in functional pathways and differentially associate with neurological disease-related genes during postnatal development. *Front. Mol. Neurosci.* **10**, 331 (2017).
45. Décarie-Spain, L. et al. Ventral hippocampus–lateral septum circuitry promotes foraging-related memory. *Cell Rep.* **40**, 111402 (2022).
46. McDougle, M. et al. Separate gut-brain circuits for fat and sugar reinforcement combine to promote overeating. *Cell Metab.* **36**, 393–407 (2024).
47. Suarez, A. N. et al. Gut vagal sensory signaling regulates hippocampus function through multi-order pathways. *Nat. Commun.* **9**, 2181 (2018).
48. Davis, E. A. et al. Ghrelin signaling affects feeding behavior, metabolism, and memory through the vagus nerve. *Curr. Biol.* **30**, 4510–4518 (2020).
49. Gentilcore, D. et al. Effects of fat on gastric emptying of and the glycemic, insulin, and incretin responses to a carbohydrate meal in type 2 diabetes. *J. Clin. Endocrinol. Metab.* **91**, 2062–2067 (2006).
50. McHugh, P. R. & Moran, T. H. Calories and gastric emptying: a regulatory capacity with implications for feeding. *Am. J. Physiol.* **236**, R254–R260 (1979).
51. Tan, H. E. et al. The gut–brain axis mediates sugar preference. *Nature* **580**, 511–516 (2020).
52. Pool, A. H. et al. The cellular basis of distinct thirst modalities. *Nature* **588**, 112–117 (2020).
53. Allen, W. E. et al. Thirst-associated preoptic neurons encode an aversive motivational drive. *Science* **357**, 1149–1155 (2017).
54. Madisen, L. et al. A robust and high-throughput Cre reporting and characterization system for the whole mouse brain. *Nat. Neurosci.* **13**, 133–140 (2010).
55. Madisen, L. et al. A toolbox of Cre-dependent optogenetic transgenic mice for light-induced activation and silencing. *Nat. Neurosci.* **15**, 793–802 (2012).
56. Rolls, B. J., Rolls, E. T., Rowe, E. A. & Sweeney, K. Sensory specific satiety in man. *Physiol. Behav.* **27**, 137–142 (1981).
57. Havermans, R. C. Stimulus specificity but no dishabituation of sensory-specific satiety. *Appetite* **58**, 852–855 (2012).
58. Yang, C. F. et al. Sexually dimorphic neurons in the ventromedial hypothalamus govern mating in both sexes and aggression in males. *Cell* **153**, 896–909 (2013).
59. Farrell, M. S. et al. A Gαs DREADD mouse for selective modulation of cAMP production in striatopallidal neurons. *Neuropsychopharmacology* **38**, 854–862 (2013).
60. O'Keefe, J. & Dostrovsky, J. The hippocampus as a spatial map: preliminary evidence from unit activity in the freely-moving rat. *Brain Res.* **34**, 171–175 (1971).
61. Tryon, V. L. et al. Hippocampal neural activity reflects the economy of choices during goal-directed navigation. *Hippocampus* **27**, 743–758 (2017).
62. Gauthier, J. L. & Tank, D. W. A dedicated population for reward coding in the hippocampus. *Neuron* **99**, 179–193 (2018).
63. Ólafsdóttir, H. F., Barry, C., Saleem, A. B., Hassabis, D. & Spiers, H. J. Hippocampal place cells construct reward related sequences through unexplored space. *eLife* **4**, e06063 (2015).
64. Martínez, M. C., Villar, M. E., Ballarini, F. & Viola, H. Retroactive interference of object-in-context long-term memory: role of dorsal hippocampus and medial prefrontal cortex. *Hippocampus* **24**, 1482–1492 (2014).
65. Leszczynski, M. How does hippocampus contribute to working memory processing? *Front. Hum. Neurosci.* **5**, 168 (2011).
66. Bird, C. M. & Burgess, N. The hippocampus and memory: insights from spatial processing. *Nat. Rev. Neurosci.* **9**, 182–194 (2008).
67. Berthoud, H.-R., Morrison, C. D., Ackroff, K. & Sclafani, A. Learning of food preferences: mechanisms and implications for obesity & metabolic diseases. *Int. J. Obes.* **45**, 2156–2168 (2021).
68. Li, M. et al. Gut–brain circuits for fat preference. *Nature* **610**, 722–730 (2022).
69. Sclafani, A. Sucrose motivation in sweet "sensitive" (C57BL/6J) and "subsensitive" (129P3/J) mice measured by progressive ratio licking. *Physiol. Behav.* **87**, 734–744 (2006).
70. Tracy, A. L., Jarrard, L. E. & Davidson, T. L. The hippocampus and motivation revisited: appetite and activity. *Behav. Brain Res.* **127**, 13–23 (2001).
71. Hodos, W. Progressive ratio as a measure of reward strength. *Science* **134**, 943–944 (1961).
72. Stewart, W. J. Progressive reinforcement schedules: a review and evaluation. *Aust. J. Psychol.* **27**, 9–22 (1975).

73. Hatori, M. et al. Time-restricted feeding without reducing caloric intake prevents metabolic diseases in mice fed a high-fat diet. *Cell Metab.* **15**, 848–860 (2012).
74. Chaix, A., Zarrinpar, A., Miu, P. & Panda, S. Time-restricted feeding is a preventative and therapeutic intervention against diverse nutritional challenges. *Cell Metab.* **20**, 991–1005 (2014).
75. Higgs, S. Cognitive influences on food intake: the effects of manipulating memory for recent eating. *Physiol. Behav.* **94**, 734–739 (2008).
76. Suzanne, H. & Jason, T. Social influences on eating. *Curr. Opin. Behav. Sci.* **9**, 1–6 (2016).
77. Clifton, P. G., Vickers, S. P. & Somerville, E. M. Little and often: ingestive behavior patterns following hippocampal lesions in rats. *Behav. Neurosci.* **112**, 502–511 (1998).
78. Briggs, S. et al. Postmeal optogenetic inhibition of dorsal hippocampal principal neurons increases future intake in a time-dependent manner. *Neurobiol. Learn. Mem.* **183**, 107478 (2021).
79. Sweeney, P. & Yang, Y. An excitatory ventral hippocampus to lateral septum circuit that suppresses feeding. *Nat. Commun.* **6**, 10188 (2015).
80. Hsu, T. M., Hahn, J. D., Konanur, V. R., Lam, A. & Kanoski, S. E. Hippocampal GLP-1 receptors influence food intake, meal size, and effort-based responding for food through volume transmission. *Neuropsychopharmacology* **40**, 327–337 (2015).
81. Kanoski, S. E. et al. Hippocampal leptin signaling reduces food intake and modulates food-related memory processing. *Neuropsychopharmacology* **36**, 1859–1870 (2011).
82. Tsetsenis, T. et al. Midbrain dopaminergic innervation of the hippocampus is sufficient to modulate formation of aversive memories. *Proc. Natl Acad. Sci. USA* **118**, e2111069118 (2021).
83. Ito, R., Robbins, T. W., Pennartz, C. M. & Everitt, B. J. Functional interaction between the hippocampus and nucleus accumbens shell is necessary for the acquisition of appetitive spatial context conditioning. *J. Neurosci.* **28**, 6950–6959 (2008).
84. Jimenez, J. C. et al. Anxiety cells in a hippocampal–hypothalamic circuit. *Neuron* **97**, 670–683 (2018).
85. LeGates, T. A. et al. Reward behaviour is regulated by the strength of hippocampus–nucleus accumbens synapses. *Nature* **564**, 258–262 (2018).
86. Loh, E. et al. Context-specific activation of hippocampus and SN/VTA by reward is related to enhanced long-term memory for embedded objects. *Neurobiol. Learn Mem.* **134**, 65–77 (2016).
87. Liu, J.-J., Tsien, R. W. & Pang, Z. P. Hypothalamic melanin-concentrating hormone regulates hippocampus–dorsolateral septum activity. *Nat. Neurosci.* **25**, 61–71 (2022).
88. Noble, E. E. et al. Hypothalamus–hippocampus circuitry regulates impulsivity via melanin-concentrating hormone. *Nat. Commun.* **10**, 4923 (2019).
89. Wee, R. W. S. et al. Internal-state-dependent control of feeding behavior via hippocampal ghrelin signaling. *Neuron* **112**, 288–305 (2024).
90. Ronchi, G., Ryu, V., Fornaro, M. & Czaja, K. Hippocampal plasticity after a vagus nerve injury in the rat. *Neural Regen. Res.* **7**, 1055–1063 (2012).
91. Biggio, F. et al. Chronic vagus nerve stimulation induces neuronal plasticity in the rat hippocampus. *Int. J. Neuropsychopharmacol.* **12**, 1209–1221 (2009).
92. O'Leary, O. F. et al. The vagus nerve modulates BDNF expression and neurogenesis in the hippocampus. *Eur. Neuropsychopharmacol.* **28**, 307–316 (2018).
93. Ura, H. et al. Vagus nerve stimulation induced long-lasting enhancement of synaptic transmission and decreased granule cell discharge in the hippocampal dentate gyrus of urethane-anesthetized rats. *Brain Res.* **1492**, 63–71 (2013).
94. Zuo, Y., Smith, D. C. & Jensen, R. A. Vagus nerve stimulation potentiates hippocampal LTP in freely-moving rats. *Physiol. Behav.* **90**, 583–589 (2007).
95. Zhao, W. et al. Brain insulin receptors and spatial memory: correlated changes in gene expression, tyrosine phosphorylation, and signaling molecules in the hippocampus of water maze trained rats. *J. Biol. Chem.* **274**, 34893–34902 (1999).
96. Merchenthaler, I., Lane, M. & Shughrue, P. Distribution of pre-pro-glucagon and glucagon-like peptide-1 receptor messenger RNAs in the rat central nervous system. *J. Comp. Neurol.* **403**, 261–280 (1999).
97. Scott, M. M. et al. Leptin targets in the mouse brain. *J. Comp. Neurol.* **514**, 518–532 (2009).
98. Zigman, J. M., Jones, J. E., Lee, C. E., Saper, C. B. & Elmquist, J. K. Expression of ghrelin receptor mRNA in the rat and the mouse brain. *J. Comp. Neurol.* **494**, 528–548 (2006).
99. Nishimura, S. et al. Functional synergy between cholecystokinin receptors CCKAR and CCKBR in mammalian brain development. *PLoS ONE* **10**, e0124295 (2015).
100. De Vadder, F. et al. Microbiota-generated metabolites promote metabolic benefits via gut–brain neural circuits. *Cell* **156**, 84–96 (2014).
101. Borgmann, D. et al. Gut–brain communication by distinct sensory neurons differently controls feeding and glucose metabolism. *Cell Metab.* **33**, 1466–1482 (2021).
102. Goldstein, N. et al. Hypothalamic detection of macronutrients via multiple gut–brain pathways. *Cell Metab.* **33**, 676–687 (2021).
103. New, J., Krasnow, M. M., Truxaw, D. & Gaulin, S. J. C. Spatial adaptations for plant foraging: women excel and calories count. *Proc. R. Soc. B Biol. Sci.* **274**, 2679–2684 (2007).
104. Allan, K. & Allan, J. L. An obesogenic bias in women's spatial memory for high calorie snack food. *Appetite* **67**, 99–104 (2013).
105. de Vries, R., de Vet, E., de Graaf, K. & Boesveldt, S. Foraging minds in modern environments: high-calorie and savory-taste biases in human food spatial memory. *Appetite* **152**, 104718 (2020).
106. Norman, K. A. & O'Reilly, R. C. Modeling hippocampal and neocortical contributions to recognition memory: a complementary-learning-systems approach. *Psychol. Rev.* **110**, 611–646 (2003).
107. O'Reilly, R. C. & McClelland, J. L. Hippocampal conjunctive encoding, storage, and recall: avoiding a trade-off. *Hippocampus* **4**, 661–682 (1994).
108. Marr, D. Simple memory: a theory for archicortex. *Philos. Trans. R. Soc. Lond. B Biol. Sci.* **262**, 23–81 (1971).
109. Rolls, E. T. & Treves, A. Neural networks in the brain involved in memory and recall. *Prog. Brain Res.* **102**, 335–341 (1994).
110. Marr, D. A theory of cerebellar cortex. *J. Physiol.* **202**, 437–470 (1969).
111. Gold, A. E. & Kesner, R. P. The role of the CA3 subregion of the dorsal hippocampus in spatial pattern completion in the rat. *Hippocampus* **15**, 808–814 (2005).
112. Hunsaker, M. R., Rosenberg, J. S. & Kesner, R. P. The role of the dentate gyrus, CA3a, b, and CA3c for detecting spatial and environmental novelty. *Hippocampus* **18**, 1064–1073 (2008).
113. Neunuebel, J. P. & Knierim, J. J. CA3 retrieves coherent representations from degraded input: direct evidence for CA3 pattern completion and dentate gyrus pattern separation. *Neuron* **81**, 416–427 (2014).
114. Neunuebel, J. P., Yoganarasimha, D., Rao, G. & Knierim, J. J. Conflicts between local and global spatial frameworks dissociate neural representations of the lateral and medial entorhinal cortex. *J. Neurosci.* **33**, 9246–9258 (2013).
115. McHugh, T. J. et al. Dentate gyrus NMDA receptors mediate rapid pattern separation in the hippocampal network. *Science* **317**, 94–99 (2007).

116. Colgin, L. L., Moser, E. I. & Moser, M.-B. Understanding memory through hippocampal remapping. *Trends Neurosci.* **31**, 469–477 (2008).
117. Lee, H., Wang, C., Deshmukh, S. S. & Knierim, J. J. Neural population evidence of functional heterogeneity along the CA3 transverse axis: pattern completion versus pattern separation. *Neuron* **87**, 1093–1105 (2015).
118. Kyle, C. T., Stokes, J. D., Lieberman, J. S., Hassan, A. S. & Ekstrom, A. D. Successful retrieval of competing spatial environments in humans involves hippocampal pattern separation mechanisms. *eLife* **4**, e10499 (2015).
119. Stark, S. M., Stevenson, R., Wu, C., Rutledge, S. & Stark, C. E. Stability of age-related deficits in the mnemonic similarity task across task variations. *Behav. Neurosci.* **129**, 257 (2015).
120. Nakazawa, K. et al. Requirement for hippocampal CA3 NMDA receptors in associative memory recall. *Science* **297**, 211–218 (2002).
121. Leutgeb, J. K., Leutgeb, S., Moser, M.-B. & Moser, E. I. Pattern separation in the dentate gyrus and CA3 of the hippocampus. *Science* **315**, 961–966 (2007).
122. Marco, A. et al. Mapping the epigenomic and transcriptomic interplay during memory formation and recall in the hippocampal engram ensemble. *Nat. Neurosci.* **23**, 1606–1617 (2020).
123. Jaeger, B. N. et al. A novel environment-evoked transcriptional signature predicts reactivity in single dentate granule neurons. *Nat. Commun.* **9**, 3084 (2018).
124. Pettit, N. L., Yap, E.-L., Greenberg, M. E. & Harvey, C. D. Fos ensembles encode and shape stable spatial maps in the hippocampus. *Nature* **609**, 327–334 (2022).
125. Liu, X. et al. Optogenetic stimulation of a hippocampal engram activates fear memory recall. *Nature* **484**, 381–385 (2012).
126. Han, J.-H. et al. Selective erasure of a fear memory. *Science* **323**, 1492–1496 (2009).
127. Semon, R. W. & Simon, L. *The Mneme* (G. Allen & Unwin Limited, 1921).
128. Josselyn, S. A., Köhler, S. & Frankland, P. W. Finding the engram. *Nat. Rev. Neurosci.* **16**, 521–534 (2015).
129. Kitamura, T. et al. Engrams and circuits crucial for systems consolidation of a memory. *Science* **356**, 73–78 (2017).
130. Tonegawa, S., Liu, X., Ramirez, S. & Redondo, R. Memory engram cells have come of age. *Neuron* **87**, 918–931 (2015).
131. Ramirez, S. et al. Activating positive memory engrams suppresses depression-like behaviour. *Nature* **522**, 335–339 (2015).
132. Redondo, R. L. et al. Bidirectional switch of the valence associated with a hippocampal contextual memory engram. *Nature* **513**, 426–430 (2014).
133. von Frisch, K. *The Dance Language and Orientation of Bees* (Harvard University Press, 1967).
134. Collett, M. & Collett, T. S. The learning and maintenance of local vectors in desert ant navigation. *J. Exp. Biol.* **212**, 895–900 (2009).
135. Collett, M., Collett, T. S. & Wehner, R. Calibration of vector navigation in desert ants. *Curr. Biol.* **9**, 1031–1034 (1999).
136. Wolf, H. & Wehner, R. Pinpointing food sources: olfactory and anemotactic orientation in desert ants, *Cataglyphis fortis*. *J. Exp. Biol.* **203**, 857–868 (2000).
137. de Vries, R., Boesveldt, S. & de Vet, E. Human spatial memory is biased towards high-calorie foods: a cross-cultural online experiment. *Int. J. Behav. Nutr. Phys. Act.* **19**, 14 (2022).
138. Tanaka, K. Z. et al. Cortical representations are reinstated by the hippocampus during memory retrieval. *Neuron* **84**, 347–354 (2014).
139. Perry, E., Walton, K. & Lambert, K. Prevalence of Malnutrition in People with Dementia in Long-term Care: A Systematic Review and Meta-analysis. *Nutrients* **15**, 2927 (2023).
140. Fostinelli, S. et al. Eating behavior in aging and dementia: the need for a comprehensive assessment. *Front. Nutr.* **7**, 604488 (2020).
141. Cowan, N. What are the differences between long-term, short-term, and working memory? *Prog. Brain Res.* **169**, 323–338 (2008).
142. Cowan, N. Short-term memory based on activated long-term memory: a review in response to Norris (2017). *Psychol. Bull.* **145**, 822–847 (2019).
143. Cowan, N. & Chen, Z. In *How Chunks Form in Long-term Memory and Affect Short-term Memory Limits* (eds. Thorn, A. & Page, M.) 86–107 (Psychology Press, 2009).
144. Oberauer, K. Access to information in working memory: exploring the focus of attention. *J. Exp. Psychol.* **28**, 411 (2002).
145. Oberauer, K. Design for a working memory. *Psychol. Learn. Motiv.* **51**, 45–100 (2009).
146. Norris, D. Short-term memory and long-term memory are still different. *Psychol. Bull.* **143**, 992–1009 (2017).
147. Norris, D. Even an activated long-term memory system still needs a separate short-term store: a reply to Cowan (2019). *Psychol. Bull.* **145**, 848–853 (2019).
148. Brown, G. D., Neath, I. & Chater, N. A temporal ratio model of memory. *Psychol. Rev.* **114**, 539 (2007).
149. Jonides, J. et al. The mind and brain of short-term memory. *Annu. Rev. Psychol.* **59**, 193–224 (2008).
150. McElree, B. Accessing recent events. *Psychol. Learn. Motiv.* **46**, 155–200 (2006).
151. Surprenant, A. & Neath, I. In *Interactions Between Short-Term and Long-term Memory in the Verbal Domain* 1st edn. (eds. Thorn, A. & Page, M.) 16–43 (Routledge, 2009).
152. Acheson, D. J., Hamidi, M., Binder, J. R. & Postle, B. R. A common neural substrate for language production and verbal working memory. *J. Cogn. Neurosci.* **23**, 1358–1367 (2011).
153. Cameron, K. A., Haarmann, H. J., Grafman, J. & Ruchkin, D. S. Long-term memory is the representational basis for semantic verbal short-term memory. *Psychophysiology* **42**, 643–653 (2005).
154. D'Esposito, M. & Postle, B. R. The cognitive neuroscience of working memory. *Annu. Rev. Psychol.* **66**, 115–142 (2015).
155. LaRocque, J. J. et al. The short-and long-term fates of memory items retained outside the focus of attention. *Mem. Cognition* **43**, 453–468 (2015).
156. Postle, B. R. Working memory as an emergent property of the mind and brain. *Neuroscience* **139**, 23–38 (2006).
157. Ranganath, C. & Blumenfeld, R. S. Doubts about double dissociations between short-and long-term memory. *Trends Cogn. Sci.* **9**, 374–380 (2005).
158. Ruchkin, D. S., Grafman, J., Cameron, K. & Berndt, R. S. Working memory retention systems: a state of activated long-term memory. *Behav. Brain Sci.* **26**, 709–728 (2003).
159. Gourley, S. L., Lee, A. S., Howell, J. L., Pittenger, C. & Taylor, J. R. Dissociable regulation of instrumental action within mouse prefrontal cortex. *Eur. J. Neurosci.* **32**, 1726–1734 (2010).
160. Corbit, L. & Balleine, B. The role of the hippocampus in instrumental conditioning. *J. Neurosci.* **20**, 4233–4239 (2000).
161. Flaherty, C. F., Coppotelli, C., Hsu, D. & Otto, T. Excitotoxic lesions of the hippocampus disrupt runway but not consummatory contrast. *Behav. Brain Res.* **93**, 1–9 (1998).
162. Karlsson, R. M., Wang, A. S., Sonti, A. N. & Cameron, H. A. Adult neurogenesis affects motivation to obtain weak, but not strong, reward in operant tasks. *Hippocampus* **28**, 512–522 (2018).

163. Krashes, M. J. et al. Rapid, reversible activation of AgRP neurons drives feeding behavior in mice. *J. Clin. Invest.* **121**, 1424–1428 (2011).
164. Stengel, A. et al. Activation of brain somatostatin 2 receptors stimulates feeding in mice: analysis of food intake microstructure. *Physiol. Behav.* **101**, 614–622 (2010).
165. Trouche, S. et al. A hippocampus-accumbens tripartite neuronal motif guides appetitive memory in space. *Cell* **176**, 1393–1406 (2019).
166. Kanatsou, S. & Krugers, H. Object-context recognition memory test for mice. *Bio-Protoc.* **6**, e1925 (2016).
167. Paxinos, G. & Franklin, K. B. J. *The Mouse Brain in Stereotaxic Coordinates* 2nd edn (Academic Press, 2001).

Acknowledgements

This study was supported by NIH grants R01 DK116004 (G.d.L.), R01 DK094871 (G.d.L.), R01 DK104897 (S.E.K.), and T32 (M.J.M.), in addition to start-up funds (G.d.L.) and an AHA predoctoral fellowship (M.X.Y.). We acknowledge R. Mendez for generously providing the brain slices used in the RNA scope analysis and J. de Lartigue for constructive comments on the manuscript.

Author contributions

Conceptualization: G.d.L. and M.Y.; Methodology: M.Y., L.D.-S., and S.E.K.; Investigation: M.Y., A.S., A.d.A., M.M., and H.E.; Writing – original draft: G.d.L.; Writing – review and editing: all authors; Funding acquisition: G.d.L., M.Y., S.E.K., and M.M.; Resources: G.d.L. and M.M.; Project administration: G.d.L.; Supervision: G.d.L.; Visualization: M.Y.; Validation: L.S.D. and S.E.K.

Competing interests

The authors declare no competing interests.

Additional information

Extended data is available for this paper at https://doi.org/10.1038/s42255-024-01194-6.

Supplementary information The online version contains supplementary material available at https://doi.org/10.1038/s42255-024-01194-6.

Correspondence and requests for materials should be addressed to Guillaume de Lartigue.

Peer review information *Nature Metabolism* thanks Guillaume Ferreira, Yingjie Zhu and the other, anonymous, reviewer(s) for their contribution to the peer review of this work. Primary Handling Editor Ashley Castellanos-Jankiewicz in collaboration with the *Nature Metabolism* team.

https://doi.org/10.1038/s42255-024-01194-6

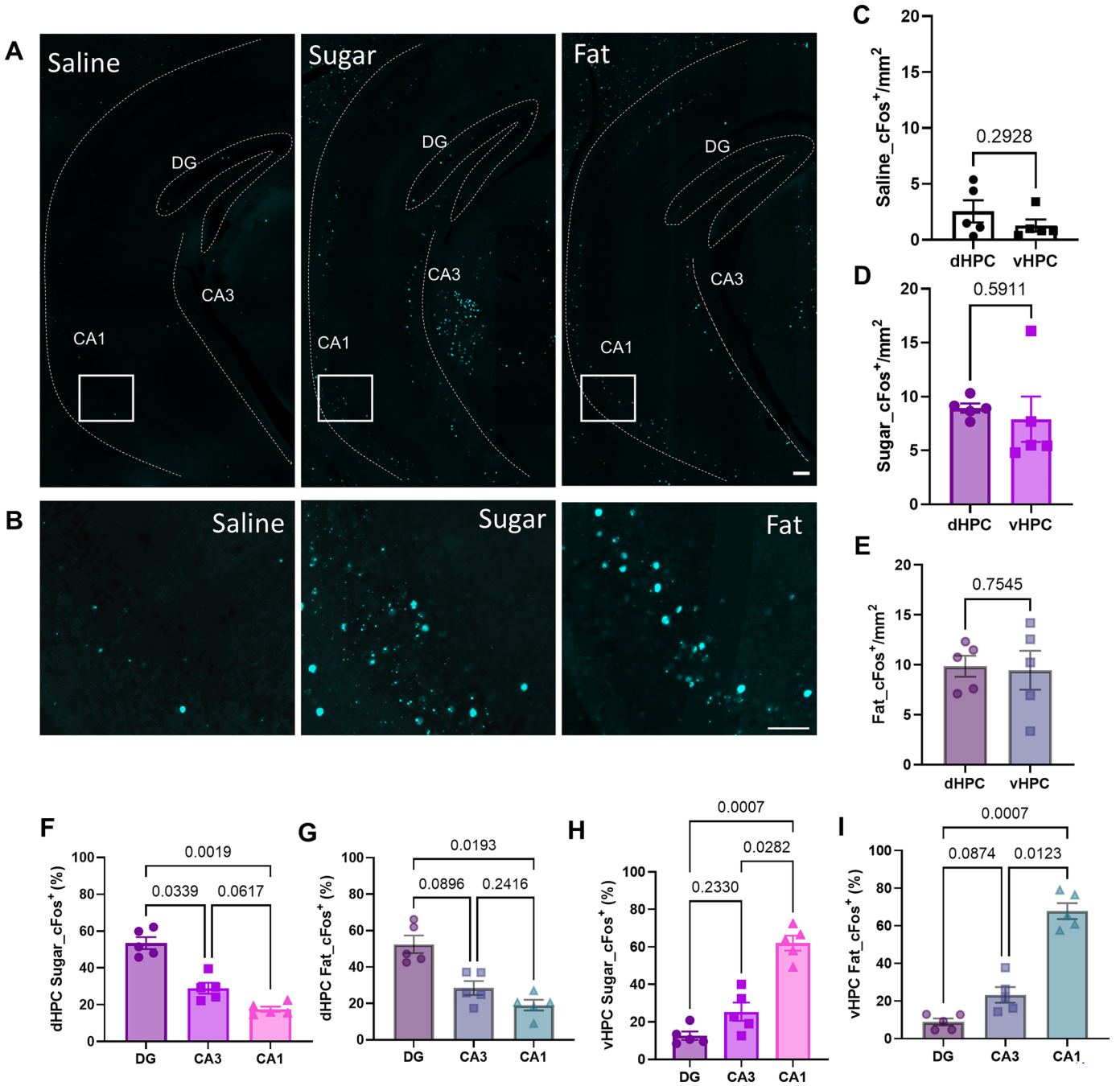

Extended Data Fig. 1 | vHPC neuronal responses to IG nutrient infusions. **A** Representative images of Fos expression in the ventral hippocampus (vHPC) following IG infusion of saline, sucrose or fat. Scale bar 100 µm **B** Higher magnification of the vCA1 from (A). Scale bar 50 µm. **C-E** Quantification of Fos-positive neurons normalized for area sized in the dHPC and vHPC following IG infusion of (**C**) saline, (**D**) sucrose or (**E**) fat. (N = 5/group, Paired Student's t test). **F-G** Relative proportion of nutrient responsive Fos-positive neurons in DG, CA3 and CA1 as a percent of the total dHPC response to IG infusion of (**F**) sucrose or (**G**) fat (N = 5/group, One-way ANOVA with Tukey post hoc analysis). **H-I** Relative proportion of nutrient responsive Fos-positive neurons in DG, CA3 and CA1 as a percent of the total vHPC response to IG infusion of (**H**) sucrose or (**I**) fat (N = 5/group, One-way ANOVA with Tukey post hoc analysis). Data are presented as mean ± s.e.m. *P < 0.05, **P < 0.01, ***P < 0.001, **** P < 0.0001, NS, not significant.

https://doi.org/10.1038/s42255-024-01194-6

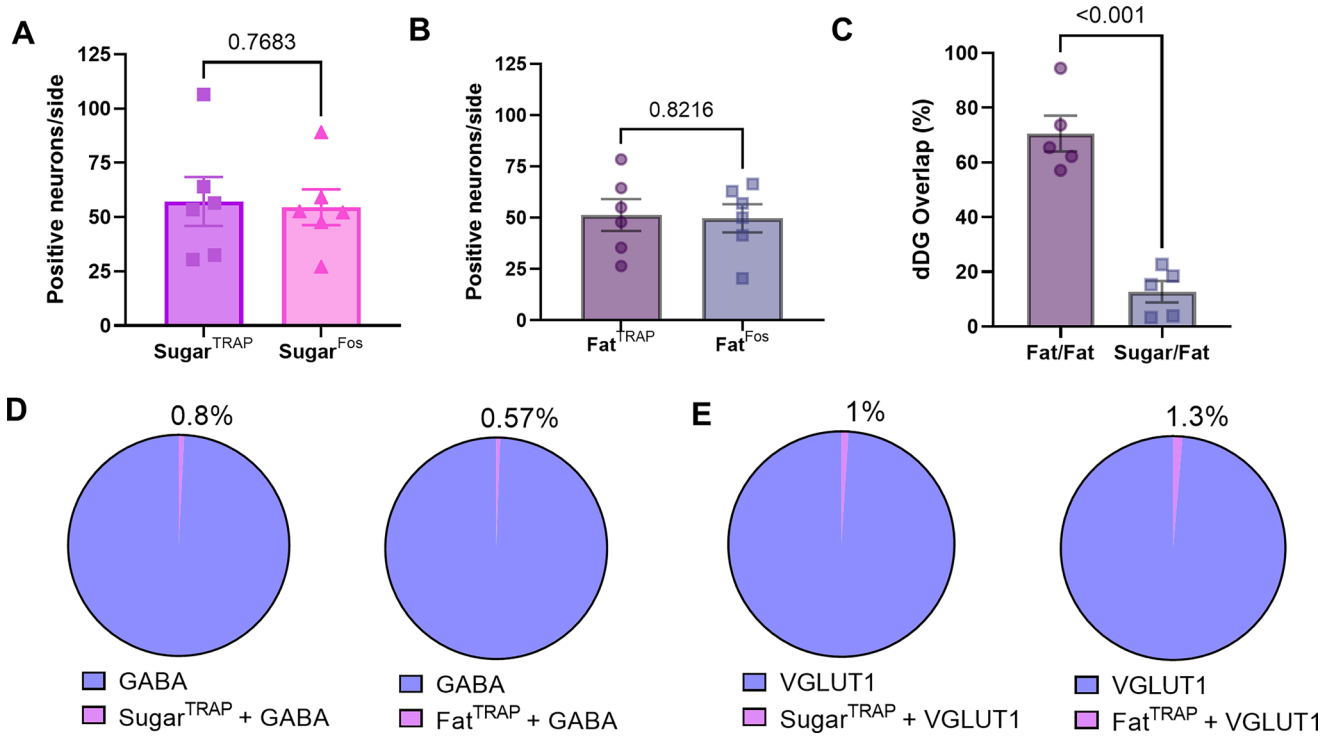

Extended Data Fig. 2 | In the absence of choice, fat responsive dHPC neurons increase fat intake independently of taste. A Number of sucrose responsive neurons in the dHPC using FosTRAP and Fos immunohistochemistry (N = 6, Paired Student's t test) **B** Number of fat responsive neurons in the dHPC using FosTRAP and Fos immunohistochemistry (N = 6, Paired Student's t test). **C** Percent overlap between neurons responding to repeated IG fat infusions compared to separate macronutrients in the dDG. (N = 5/group, unpaired t test). **D** Proportion of GABA-expressing neurons colocalized with tdTomato positive neurons trapped with IG infusion of sucrose (left) or fat (right). **E** Proportion of vGLUT1-expressing neurons colocalized with tdTomato positive neurons trapped with IG infusion of sucrose (left) or fat (right). Data are presented as mean ± s.e.m. **** $P < 0.0001$, ns, not significant.

https://doi.org/10.1038/s42255-024-01194-6

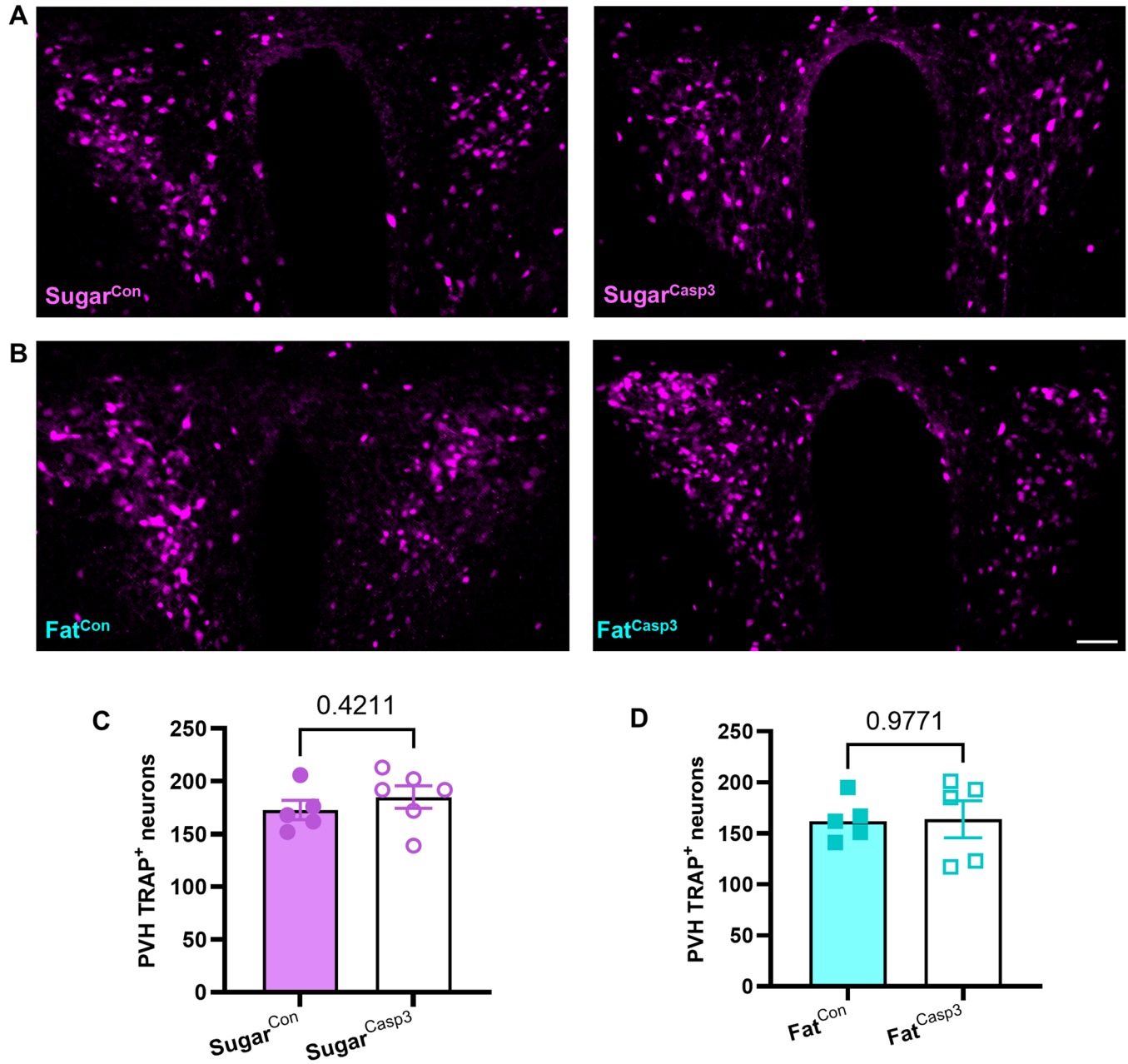

Extended Data Fig. 3 | Confirmation of dHPC specificity of caspase mediated ablation. A. Representative images of tdTomato-positive neurons in the PVH of FosTRAP mice following IG infusion of sucrose with control virus injection (left) or caspase virus injection in the dHPC. **B** Representative images of tdTomato-positive neurons in the PVH of FosTRAP mice following IG infusion of sucrose with control virus injection (left) or caspase virus injection in the dHPC. **C** Quantification of sucrose-responsive tdTomato-positive neurons in the PVH (N = 5-6, Unpaired Student's t-test). **D** Quantification of fat-responsive tdTomato-positive neurons in the PVH (N = 5, Unpaired Student's t-test). Data are presented as mean ± s.e.m. ns, not significant. Scale bars 100 µm.

https://doi.org/10.1038/s42255-024-01194-6

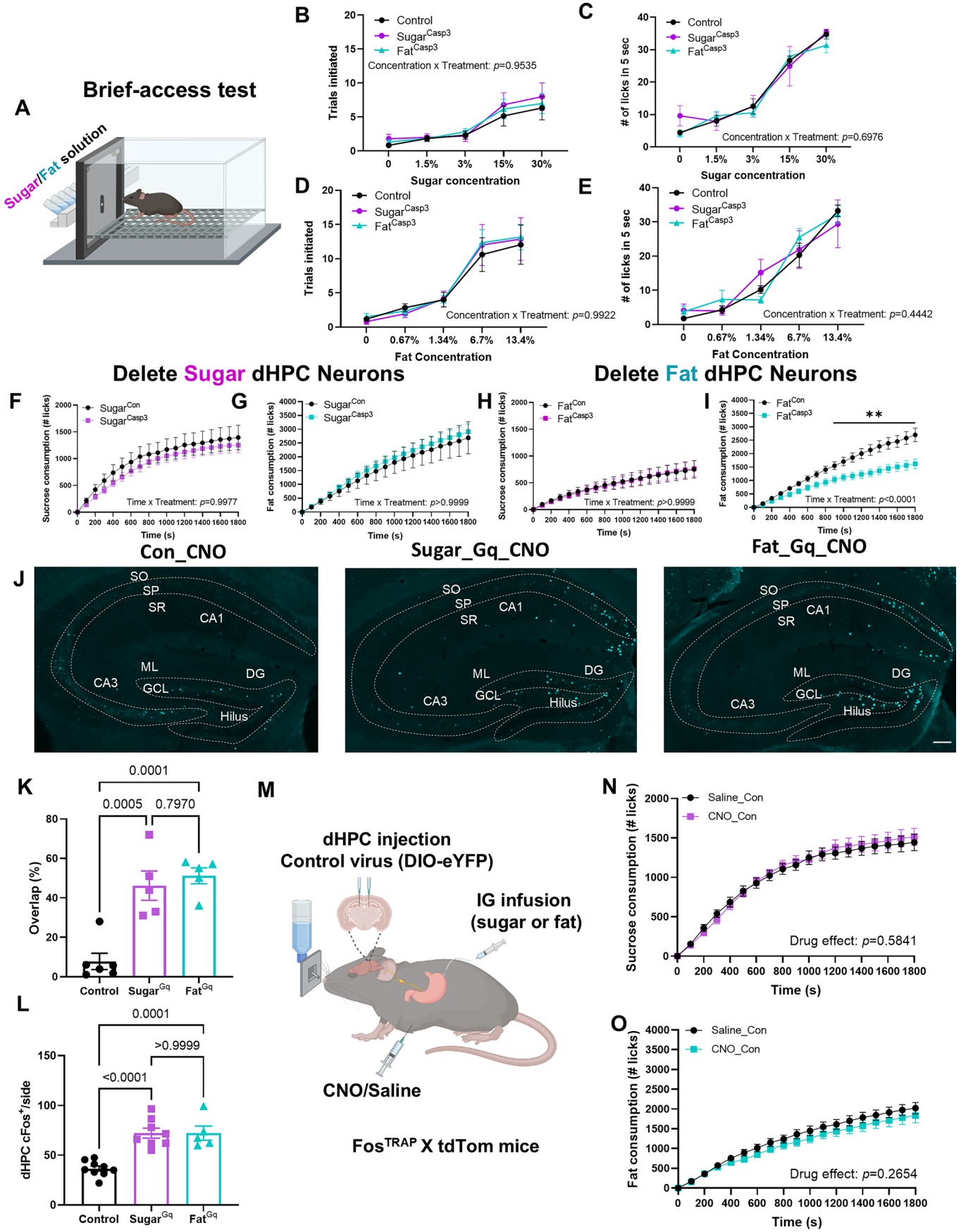

Extended Data Fig. 4 | See next page for caption.

https://doi.org/10.1038/s42255-024-01194-6

Extended Data Fig. 4 | Fat and sugar responsive dHPC neurons influence intake in a nutrient-specific manner and have no effect on taster. A. Schematic of Davis rig for brief access taste preference test. **B** Trials initiated for a range sucrose concentrations in Fos^{TRAP} mice with ablation of $dHPC^{Sugar}$, $dHPC^{Fat}$, or controls (N = 5-6/group, Two-way ANOVA with Holm-Sidak post-hoc analysis). **C** Number of licks in the first 5 s per trial for a range sucrose concentrations in Fos^{TRAP} with ablation of $dHPC^{Sugar}$, $dHPC^{Fat}$, or controls (N = 5-6/group, Two-way ANOVA with Holm-Sidak post-hoc analysis). **D** Trials initiated for a range fat concentrations in Fos^{TRAP} mice with ablation of $dHPC^{Sugar}$, $dHPC^{Fat}$, or controls (N = 5-6/group, Two-way ANOVA with Holm-Sidak post-hoc analysis). **E** Number of licks per 5 s trial for a range fat concentrations in FosTRAP mice with ablation of $dHPC^{Sugar}$, $dHPC^{Fat}$, or controls (N = 5-6/group, Two-way ANOVA with Holm-Sidak post-hoc analysis). **F-I** Lick numbers (1ul/lick) of sucrose or fat solutions when presented as a single bottle with no choice. (**F**) Sucrose solution licking in $dHPC^{Sugar}$ mice with and without viral-mediated ablation (N = 8-9/group, Two-way ANOVA with Holm-Sidak post hoc analysis). (**G**) Fat solution licking in $dHPC^{Sugar}$ mice with and without viral-mediated ablation (N = 8-9/group, Two-way ANOVA with Holm-Sidak post hoc analysis). (**H**) Sucrose solution licking in $dHPC^{Fat}$ mice with and without viral-mediated ablation (N = 8/group, Two-way ANOVA with Holm-Sidak post hoc analysis). (**I**) Fat solution licking in $dHPC^{Fat}$ mice with and without viral-mediated ablation (N = 8/group, Two-way ANOVA with Holm-Sidak post hoc analysis). **J** Representative images of CNO-induced Fos expression (cyan) in dHPC of control FosTRAP mice or mice expressing hM3Dq in $dHPC^{Sugar}$ or $dHPC^{Fat}$ neurons**. K** Percent overlap of CNO induced cFos in tdtomato-positive TRAP neurons (N = 5-6/group, One-way ANOVA with Tukey post hoc analysis). **L** Number of CNO induced cFos-positivie neurons (N = 5-9/group, One-way ANOVA with Tukey post hoc analysis). **M** Schematic of the Fos^{TRAP} mice that receive a virus expressing YFP reporter to serve as a negative control for the chemogenetic experiment in Fig. 3. **N** Sucrose solution licking in control mice following saline or CNO (N = 11/group, Two-way ANOVA with Holm-Sidak post hoc analysis). **O** Fat solution licking in control mice following saline or CNO (N = 10/group, Two-way ANOVA with Holm-Sidak post hoc analysis). Data are presented as mean ± s.e.m. **P < 0.01, ***P < 0.001, ns, not significant. Scale bars 100 µm. Elements of this figure were created in BioRender. Lab, D. (2024) BioRender.com/i72i182.

https://doi.org/10.1038/s42255-024-01194-6

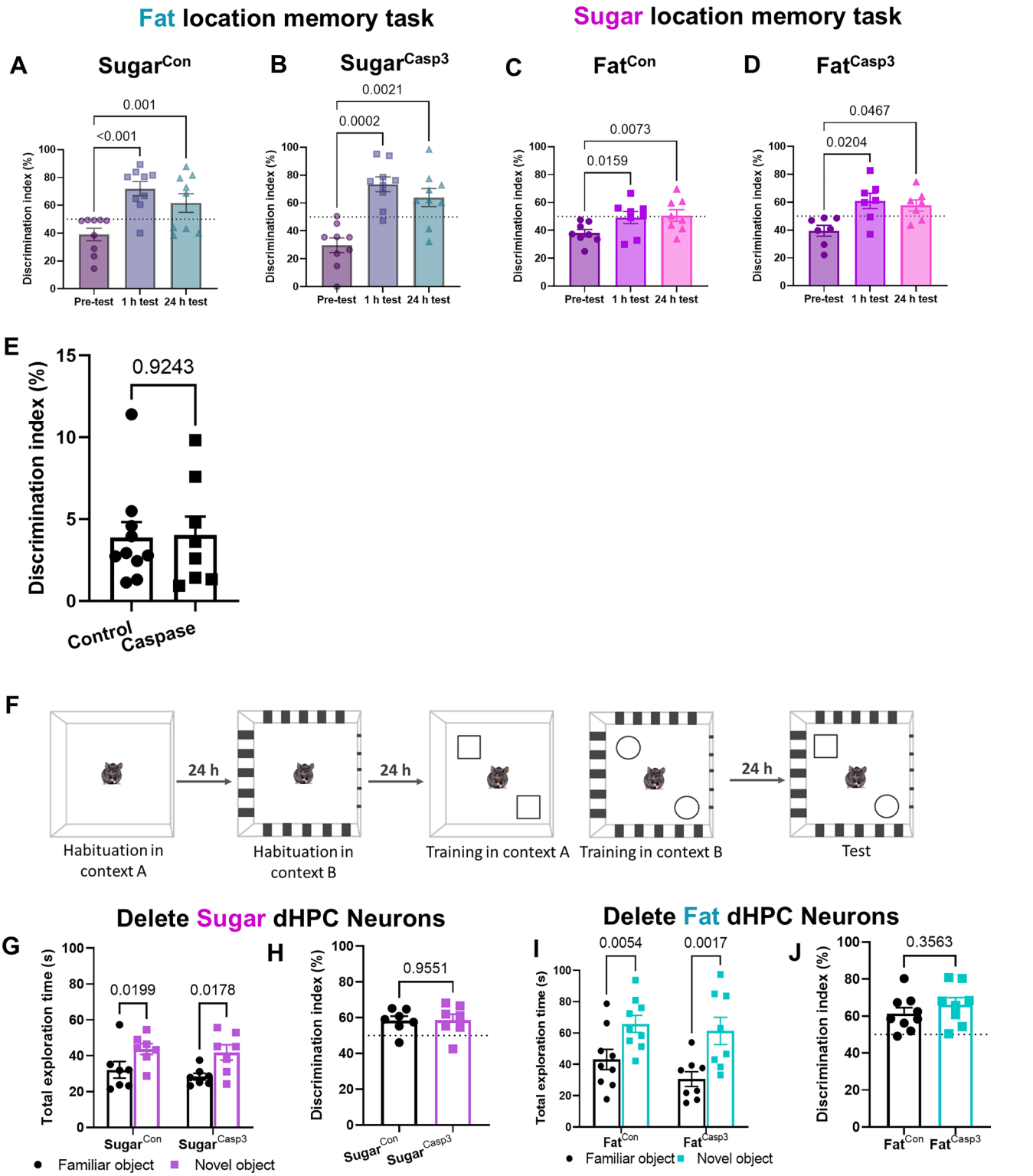

Extended Data Fig. 5 | Ablation of nutrient responsive dHPC neurons has no effect on memory recall of different nutrient location or non-food related memory. A-E Control experiments for Fig. 4. **(A)** Discrimination of fat quadrant in dHPC^{Sugar} mice without viral-mediated ablation (N = 9, One-way ANOVA with Tukey post hoc analysis). **(B)** Discrimination of fat quadrant in dHPC^{Sugar} mice with viral-mediated ablation (N = 9, One-way ANOVA with Tukey post hoc analysis). **(C)** Discrimination of sucrose quadrant in dHPC^{Fat} mice without viral-mediated ablation (N = 8/group, One-way ANOVA with Tukey post hoc analysis). **(D)** Discrimination of sucrose quadrant in dHPC^{Fat} mice with viral-mediated ablation (N = 8/group, One-way ANOVA with Tukey post hoc analysis). **E** Discrimination index of the nutrient-paired quadrant one week after the training (N = 8-10/group, Unpaired Student's t-test). **F** Schematic of novel object in context. **G** Exploration time of familiar and novel object on test day in dHPC^{Sugar} mice with and without viral-mediated ablation (N = 7/group, Two-way ANOVA with Holm-Sidak post hoc analysis). **H** Percent of the time spent exploring the object that is novel in new context in the same animals (N = 7, Unpaired Student's t-test). **I** Exploration time of familiar and novel object on test day in in dHPC^{Fat} mice with and without viral-mediated ablation (N = 8-9/group, Two-way ANOVA with Holm-Sidak post hoc analysis). **J** Percent of the time spent exploring the object that is novel in new context in the same animals (N = 8-9, Unpaired Student's t-test).

https://doi.org/10.1038/s42255-024-01194-6

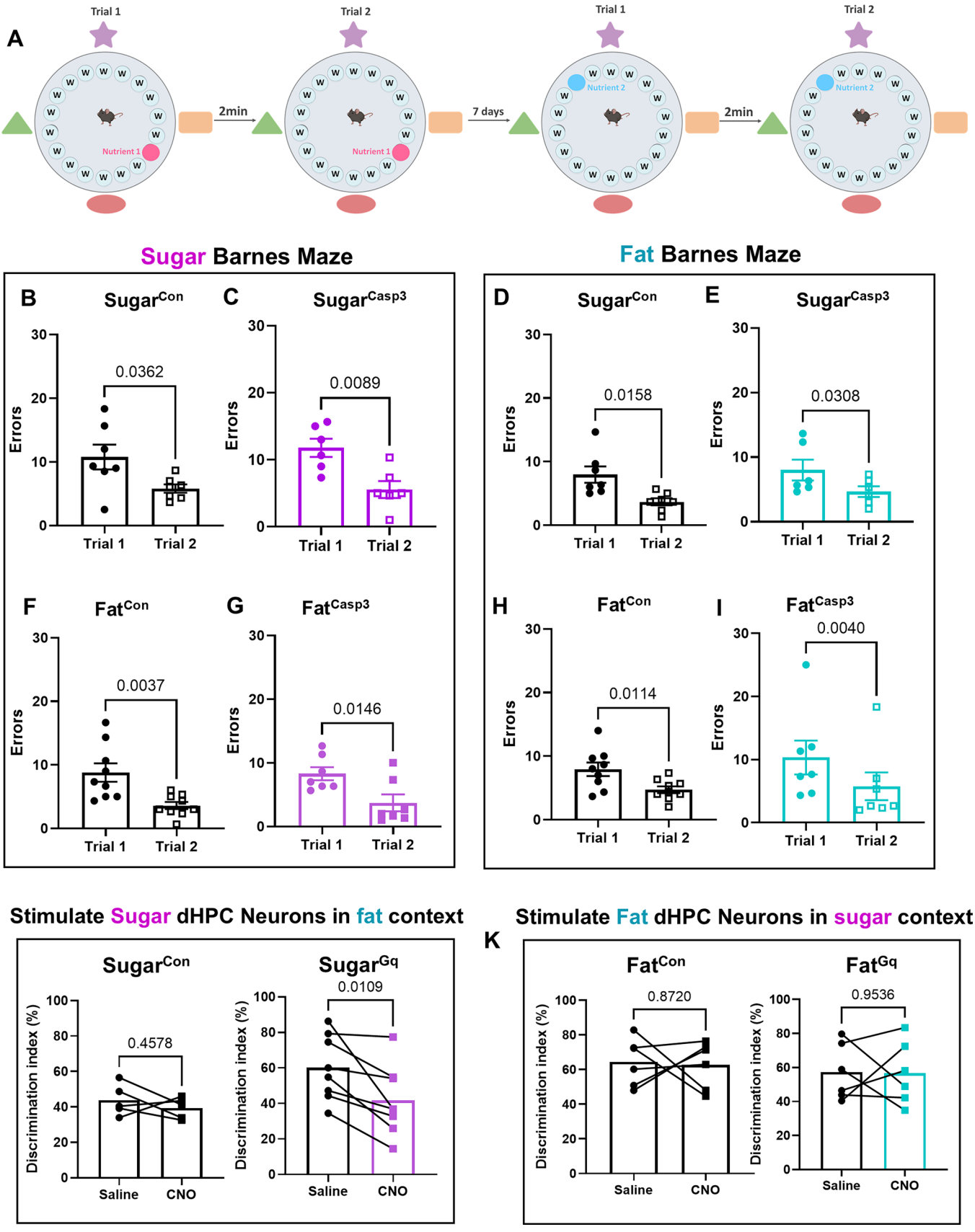

Extended Data Fig. 6 | See next page for caption.

https://doi.org/10.1038/s42255-024-01194-6

Extended Data Fig. 6 | Fat- and sucrose-responsive dHPC neurons are not required for working memory or sufficient to influence memory in the wrong context. A Schematic of nutrient-related Barnes maze test. **B** Number of errors in locating the sucrose location on first and second trial in $dHPC^{Sugar}$ mice without viral-mediated ablation (N = 7/group, Paired Student's t test). **C** Number of errors in locating the sucrose location on first and second trial in $dHPC^{Sugar}$ mice with viral-mediated ablation (N = 6/group, Paired Student's t test). **D** Number of errors in locating the fat location on first and second trial in $dHPC^{Sugar}$ mice without viral-mediated ablation (N = 7/group, Paired Student's t test). **E** Number of errors in locating the fat location on first and second trial in $dHPC^{Sugar}$ mice with viral-mediated ablation (N = 6/group, Paired Student's t test). **F** Number of errors in locating the sucrose location on first and second trial in $dHPC^{Fat}$ mice without viral-mediated ablation (N = 9/group, Paired Student's t test). **G** Number of errors in locating the sucrose location on first and second trial in $dHPC^{Fat}$ mice with viral-mediated ablation (N = 7/group, Paired Student's t test). **H** Number of errors in locating the fat location on first and second trial in $dHPC^{Fat}$ mice without viral-mediated ablation (N = 9/group, Paired Student's t test). **I** Number of errors in locating the fat location on first and second trial in $dHPC^{Fat}$ mice with viral-mediated ablation (N = 7/group, Paired Student's t test). **J** Control experiment for Fig. 4g. Discrimination of fat quadrant in response to saline and CNO in $dHPC^{Sugar}$ mice expressing viral-mediated hM3Dq or control (N = 5-8/group, Paired Student's t test). **K** Control experiment for Fig. 4h. Discrimination of sucrose quadrant in response to saline and CNO in $dHPC^{Fat}$ mice expressing viral-mediated hM3Dq or control (N = 6-7/group, Paired Student's t test). Data are presented as mean ± s.e.m. *P < 0.05, **P < 0.01, ns, not significant. Elements of this figure were created in BioRender. Lab, D. (2024) BioRender.com/c40u835.

https://doi.org/10.1038/s42255-024-01194-6

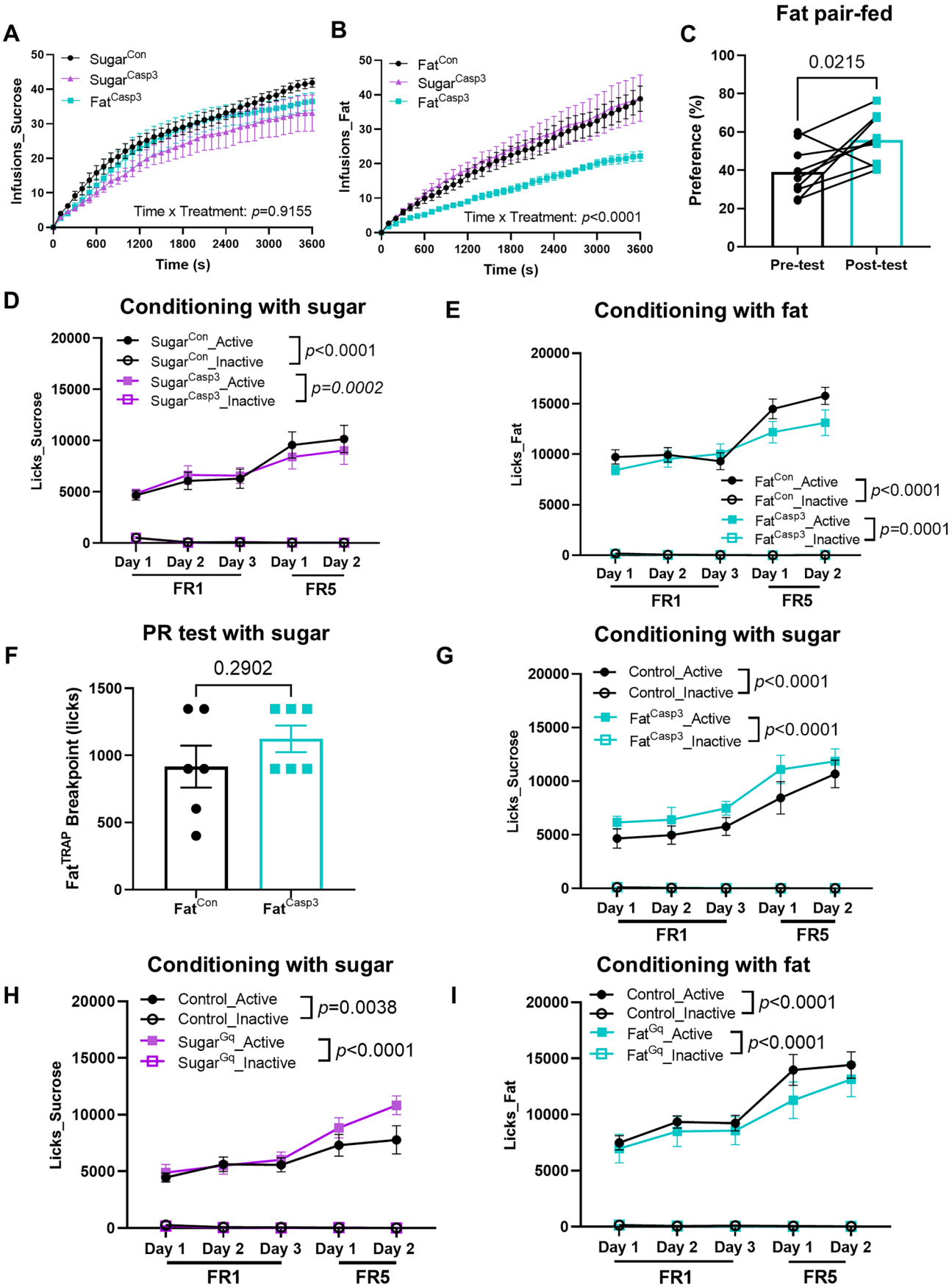

Extended Data Fig. 7 | See next page for caption.

https://doi.org/10.1038/s42255-024-01194-6

Extended Data Fig. 7 | Fat- and sucrose-responsive dHPC neurons are not required for learning. A Number of sucrose infusions received during conditioning tests from Fig. 5b, c and f (N = 6-8, Two-way ANOVA with Holm-Sidak post hoc analysis). **B.** Number of fat infusions received during conditioning tests from Fig. 5b, c and f (N = 5-7, Two-way ANOVA with Holm-Sidak post hoc analysis). **C** Preference for fat paired flavor after restricting conditioning infusions in control mice to match the number of ablation of fat-responsive dHPC neurons (N = 9/group, Paired Student's t test). **D** Sucrose lick number for active and inactive sippers during conditioning session for $dHPC^{Sugar}$ mice with control or caspase virus (N = 7, Two-way ANOVA with Holm-Sidak post hoc analysis). **E** Fat lick number for active and inactive sippers during conditioning session for $dHPC^{Fat}$ mice with control or caspase virus (N = 9-10, Two-way ANOVA with Holm-Sidak post hoc analysis). **F** Breakpoint for sucrose reward in $dHPC^{Fat}$ mice with control or caspase virus (N = 6, Two-way ANOVA with Holm-Sidak post hoc analysis). **G** Sucrose lick number for active and inactive sippers during conditioning session for $dHPC^{Fat}$ mice with control or caspase virus (N = 6, Two-way ANOVA with Holm-Sidak post hoc analysis). **H** Sucrose lick number for active and inactive sippers during conditioning session for $dHPC^{Sucrose}$ mice with control or hM3Dq virus (N = 6-11, Two-way ANOVA with Holm-Sidak post hoc analysis). **I** Fat lick number for active and inactive sippers during conditioning session for $dHPC^{Fat}$ mice with control or hM3Dq virus (N = 10-12, Two-way ANOVA with Holm-Sidak post hoc analysis). Data are presented as mean ± s.e.m. *P < 0.05, ns, not significant.

https://doi.org/10.1038/s42255-024-01194-6

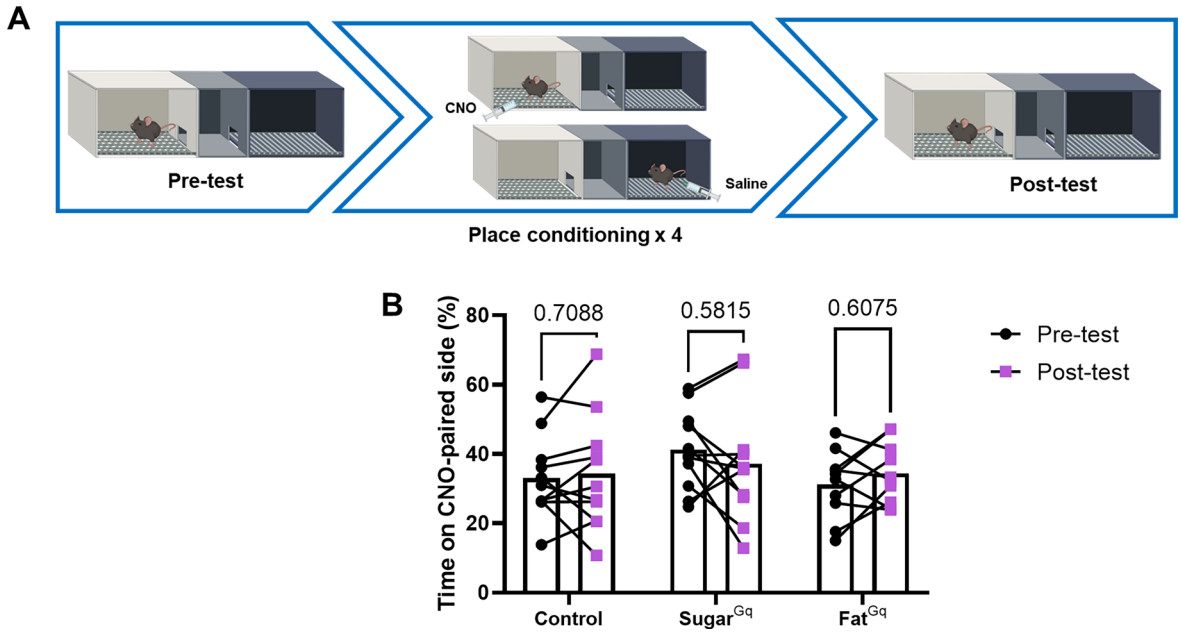

Extended Data Fig. 8 | Motivation induced by nutrient-responsive dHPC neurons is tied to food-related context. A Schematic of conditioned place preference paradigm. **B** CNO paired flavor preference pre and post conditioning in control Fos^{TRAP} mice, or mice expressing hM3Dq in $dHPC^{Sugar}$ or $dHPC^{Fat}$ neurons (N = 10-11/group, Two-way ANOVA with Holm-Sidak post hoc analysis). Elements of this figure were created in BioRender. Lab, D. (2024) BioRender.com/w97b713.

https://doi.org/10.1038/s42255-024-01194-6

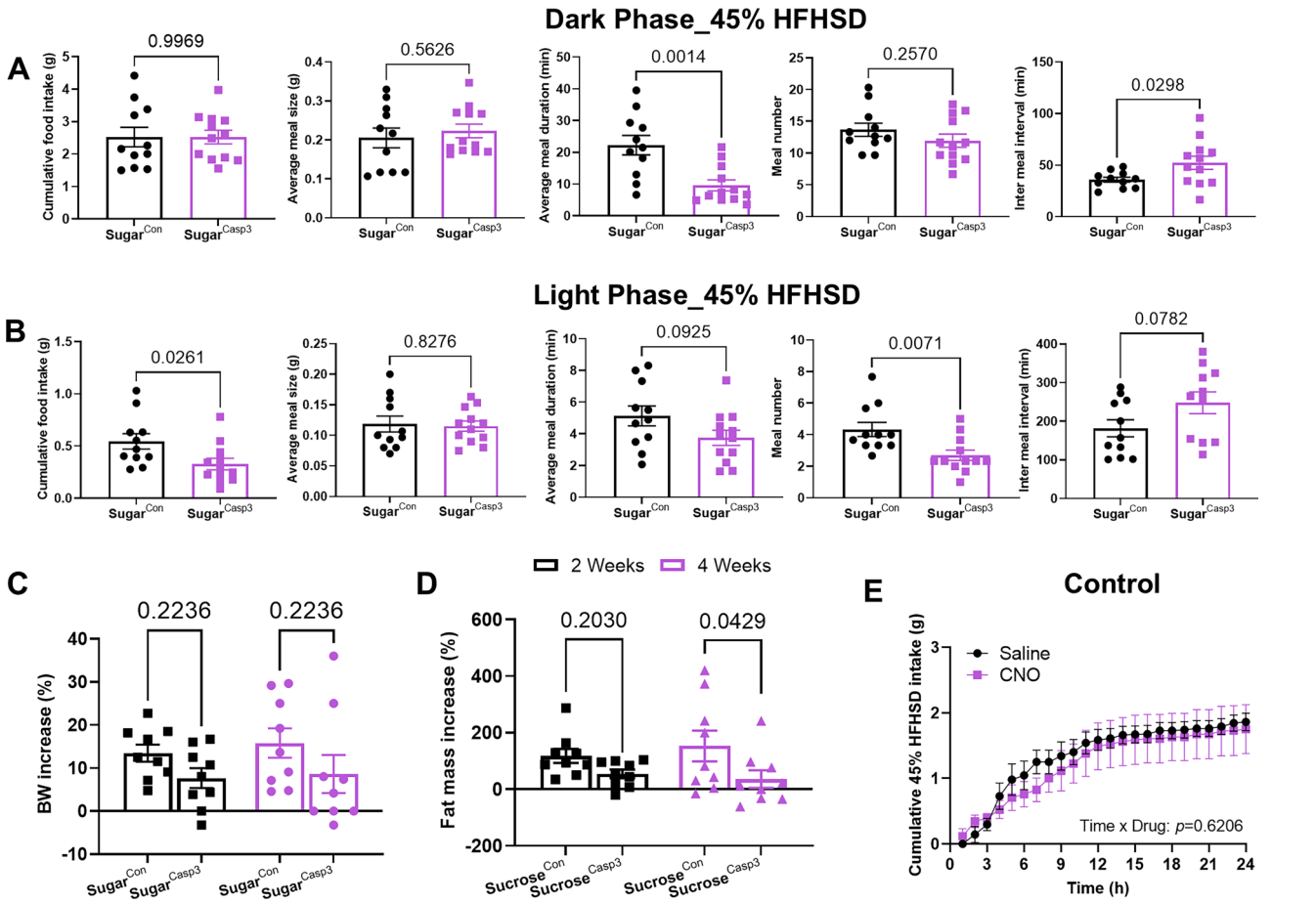

Extended Data Fig. 9 | Deletion of dHPC^{Sugar} neurons decreases meal number in the dark phase and prevents weight gain over 4 weeks. A Dark phase meal pattern analysis of 45% HFHS diet in dHPC^{Sugar} mice with viral-mediated ablation (N = 11-12/group, unpaired t-test). **B** Light phase meal pattern analysis of 45% HFHS diet in dHPC^{Sugar} mice with viral-mediated ablation (N = 11-12/group, unpaired t-test). **C** Comparing percent weight gain at 2 and 4 weeks between dHPC^{Sugar} mice with viral-mediated ablation (N = 9/group, two-way ANOVA with Holm-Sidak post hoc analysis). **D** Comparing percent fat mass accumulation at 2 and 4 weeks between dHPC^{Sugar} mice with viral-mediated ablation (N = 9/group, two-way ANOVA with Holm-Sidak post hoc analysis). **E** Cumulative hourly food intake in control mice in response to saline and CNO (N = 5, Two-way RM ANOVA with Holm-Sidak post-hoc analysis).

https://doi.org/10.1038/s42255-024-01194-6

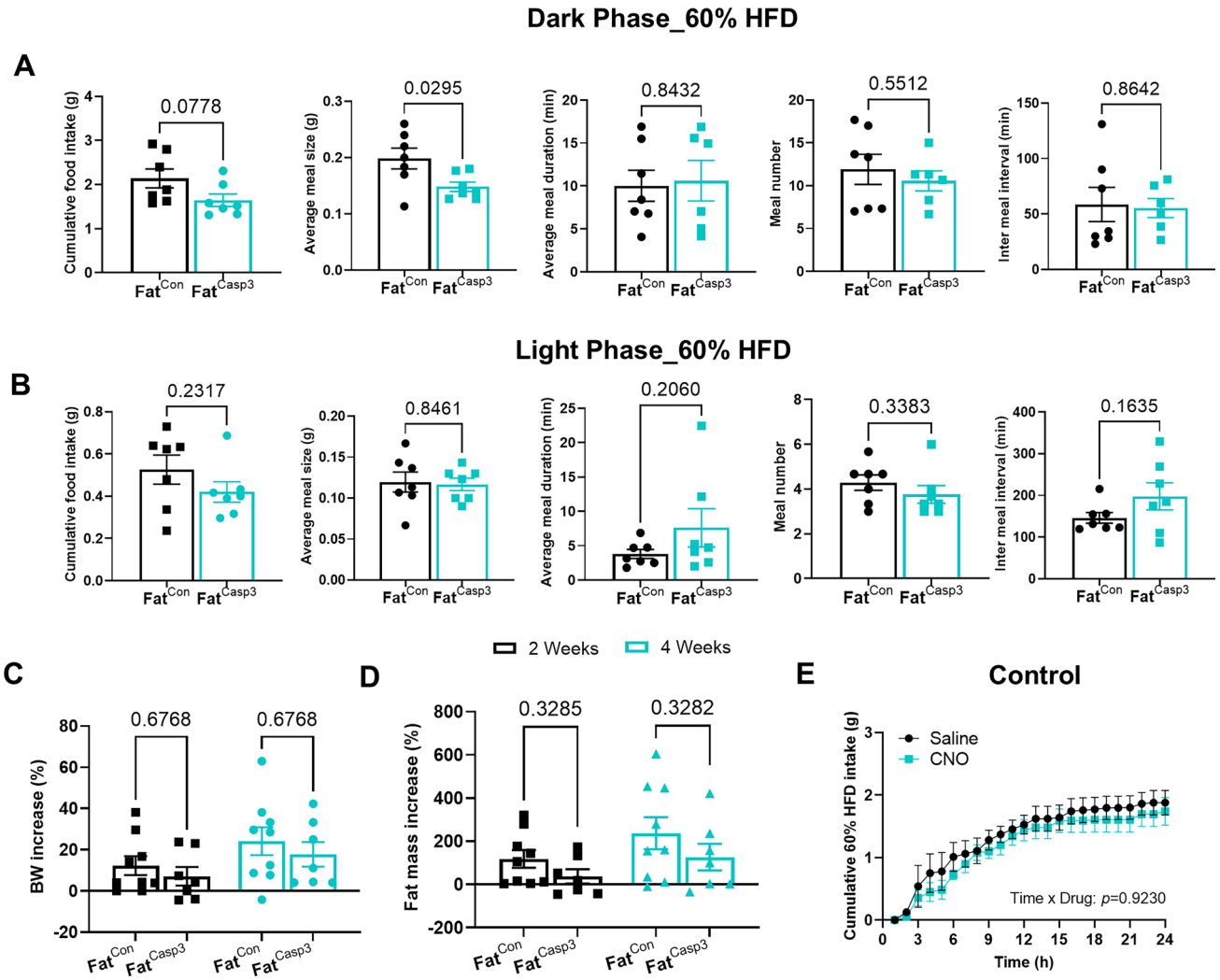

Extended Data Fig. 10 | Deletion of dHPC^{Fat} neurons decreases meal size in the dark phase. A Dark phase meal pattern analysis of 45% HFHS diet in dHPC^{Sugar} mice with viral-mediated ablation (N = 11-12/group, Unpaired Student's t test). **B** Light phase meal pattern analysis of 45% HFHS diet in dHPC^{Sugar} mice with viral-mediated ablation (N = 11-12/group, Unpaired Student's t test). **C** Comparing percent weight gain at 2 and 4 weeks between dHPC^{Sugar} mice with viral-mediated ablation (N = 9/group, Two-way ANOVA with Holm-Sidak post hoc analysis). **D** Comparing percent fat mass accumulation at 2 and 4 weeks between dHPC^{Sugar} mice with viral-mediated ablation (N = 9/group, Two-way ANOVA with Holm-Sidak post hoc analysis). **E** Cumulative hourly food intake in control mice in response to saline and CNO (N = 5, Two-way RM ANOVA with Holm-Sidak post-hoc analysis).

nature portfolio

Corresponding author(s): Guillaume de Lartigue

Last updated by author(s): Sep 20, 2024

Reporting Summary

Nature Portfolio wishes to improve the reproducibility of the work that we publish. This form provides structure for consistency and transparency in reporting. For further information on Nature Portfolio policies, see our Editorial Policies and the Editorial Policy Checklist.

Statistics

For all statistical analyses, confirm that the following items are present in the figure legend, table legend, main text, or Methods section.

n/a	Confirmed
☐	☒ The exact sample size (*n*) for each experimental group/condition, given as a discrete number and unit of measurement
☐	☒ A statement on whether measurements were taken from distinct samples or whether the same sample was measured repeatedly
☐	☒ The statistical test(s) used AND whether they are one- or two-sided *Only common tests should be described solely by name; describe more complex techniques in the Methods section.*
☒	☐ A description of all covariates tested
☐	☒ A description of any assumptions or corrections, such as tests of normality and adjustment for multiple comparisons
☐	☒ A full description of the statistical parameters including central tendency (e.g. means) or other basic estimates (e.g. regression coefficient) AND variation (e.g. standard deviation) or associated estimates of uncertainty (e.g. confidence intervals)
☐	☒ For null hypothesis testing, the test statistic (e.g. *F*, *t*, *r*) with confidence intervals, effect sizes, degrees of freedom and *P* value noted *Give P values as exact values whenever suitable.*
☒	☐ For Bayesian analysis, information on the choice of priors and Markov chain Monte Carlo settings
☒	☐ For hierarchical and complex designs, identification of the appropriate level for tests and full reporting of outcomes
☒	☐ Estimates of effect sizes (e.g. Cohen's *d*, Pearson's *r*), indicating how they were calculated

Our web collection on statistics for biologists contains articles on many of the points above.

Software and code

Policy information about availability of computer code

Data collection	Feeding data were collected from a BioDAQ system using Biodaq Monitoring Software. Reward behavioral data and licking data were acquired using Med Associates chambers and were collected using proprietary Med PC-V Software Suite. Gustometer measurements were acquired with Davis rig MS-160 from DiLog Instruments (now MedAssociates) using proprietary DavisRig software. The memory behavioral data were acquired using proprietary EthoVision XT (version 17) software. Immunofluorescence images were captured using a Keyence microscope and quantification performed using proprietary NIS Elements AR Analysis software (version 5.11.01). Whole nodose ganglia were imaged with Bruker 2 photon Ultima 2Pplus microscope using proprietary Prairie View Software version 5.7.
Data analysis	Data were analyzed using Graphpad Prism version 10

For manuscripts utilizing custom algorithms or software that are central to the research but not yet described in published literature, software must be made available to editors and reviewers. We strongly encourage code deposition in a community repository (e.g. GitHub). See the Nature Portfolio guidelines for submitting code & software for further information.

Data

Policy information about availability of data

All manuscripts must include a data availability statement. This statement should provide the following information, where applicable:

- Accession codes, unique identifiers, or web links for publicly available datasets
- A description of any restrictions on data availability
- For clinical datasets or third party data, please ensure that the statement adheres to our policy

There are no publicly available datasets for this manuscript. All data necessary to interpret, replicate and build upon the methods or findings reported here are contained within the manuscript and supplemental information. All mouse lines, plasmids and reagents used in this study have been previously published and/or are commercially available, and are detailed in the Reporting Summary. The Mouse Brain Atlas utilized to identified regions of the brain is George Paxinos' and Keith B.J. Franklin's The Mouse Brain in Stereotaxic Coordinates, Second Edition, published in July 2001 by Academic Press. Further information and requests for resources and reagents should be directed to and will be fulfilled by Dr de Lartigue.

Research involving human participants, their data, or biological material

Policy information about studies with human participants or human data. See also policy information about sex, gender (identity/presentation), and sexual orientation and race, ethnicity and racism.

Reporting on sex and gender	N/A
Reporting on race, ethnicity, or other socially relevant groupings	N/A
Population characteristics	N/A
Recruitment	N/A
Ethics oversight	N/A

Note that full information on the approval of the study protocol must also be provided in the manuscript.

Field-specific reporting

Please select the one below that is the best fit for your research. If you are not sure, read the appropriate sections before making your selection.

☒ Life sciences ☐ Behavioural & social sciences ☐ Ecological, evolutionary & environmental sciences

For a reference copy of the document with all sections, see nature.com/documents/nr-reporting-summary-flat.pdf

Life sciences study design

All studies must disclose on these points even when the disclosure is negative.

Sample size	Data Formal sample size calculations were performed based on pilot data.
exclusions	Data from all animals with histologically confirmed viral expression were included in analysis
Replication	All behavioral and imaging experiments were repeated in at least two separate cohorts of animals, with the exception of the body weight experiments in the last figure which were only done in one cohort. All attempts at replication were successful
Randomization	All experiments were performed in pseudo random counterbalanced design with all animals receiving each treatment
Blinding	All data were analyzed by investigators blinded to the treatment conditions. Investigators were not blinded to group allocations.

Reporting for specific materials, systems and methods

We require information from authors about some types of materials, experimental systems and methods used in many studies. Here, indicate whether each material, system or method listed is relevant to your study. If you are not sure if a list item applies to your research, read the appropriate section before selecting a response.

Materials & experimental systems

n/a	Involved in the study
☐	☒ Antibodies
☒	☐ Eukaryotic cell lines
☒	☐ Palaeontology and archaeology
☐	☒ Animals and other organisms
☒	☐ Clinical data
☒	☐ Dual use research of concern
☒	☐ Plants

Methods

n/a	Involved in the study
☒	☐ ChIP-seq
☒	☐ Flow cytometry
☒	☐ MRI-based neuroimaging

Antibodies

Antibodies used: Rabbit anti cFos Cell Signalling Technologies, Cat#2250; RRID: AB_2247211
Alexa Fluor 647 Donkey anti rabbit Thermo Fisher Scientific (Cat#A32795, RRID: AB_2762835)

Validation: The antibodies used have been previously used and published extensively in the model (Mouse) and applications (Brain IF) used here. Full details are available via the Resource Report ID is reported

Animals and other research organisms

Policy information about studies involving animals; ARRIVE guidelines recommended for reporting animal research, and Sex and Gender in Research

Laboratory animals: Adult male and female mice (C57Bl6) Strains: B6.129(Cg)- Fostm1.1(cre/ERT2)Luo/J (JAX stock no.021882) and Ai14 (B6.Cg-Gt(ROSA)26Sortm14(CAG-tdTomato)Hze/J, JAX stock no.007914) maintained on a reverse 12-h light/dark circle. Aged 6-20 weeks

Wild animals: No wild animals were used

Reporting on sex: Equal numbers of male and female mice were used for all experiments and data is presented as mixed data

Field-collected samples: No field collected samples were used

Ethics oversight: All experiments were performed in accordance with the US Public Health Services policy on the Humane Care and Use of Laboratory Animals and experimental protocols were approved by the Institutional Animal Care and Use Committee (IACUC) at the University of Florida (Protocol # 202110305) and Monell Chemical Senses Center (Protocol # 1187 and 1190).

Note that full information on the approval of the study protocol must also be provided in the manuscript.

Plants

Seed stocks: N/A

Novel plant genotypes: N/A

Authentication: N/A